Journal of Non-Crystalline Solids 92 (1987) 183–244
North-Holland, Amsterdam

A REVIEW OF AMORPHOUS SILICON ALLOYS
Fabrication, properties and applications

P.K. SHUFFLEBOTHAM and H.C. CARD

Materials and Devices Research Laboratory, Department of Electrical Engineering, University of Manitoba, Winnipeg, Manitoba, Canada R3T 2N2

A. THANAILAKIS

Laboratory of Electrotechnical and Electronic Materials Technology, Department of Electrical Engineering, Democritus University of Thrace, Xanthi, Greece

Received 19 February 1986
Revised manuscript received 14 January 1987

A review of amorphous silicon alloys (other than a-Si : H) is presented. The main focus is on experimental results. Methods of fabricating amorphous alloys are classified and their basic operational principles outlined. The electrical and optical properties of amorphous silicon based alloys are then described, and a summary of existing and potential applications given. Conspicuous gaps in the fabrication, understanding and application of these materials are pointed out. A comprehensive (though not exhaustive) bibliography is presented, with references to all amorphous silicon alloys studied up to the summer of 1986.

Contents

0022-3093/87/$03.50

1. Introduction

Over the span of a single decade, amorphous semiconductors have risen from almost complete obscurity to become one of the most active areas in condensed matter physics. This has largely been a result of the discovery of the hydrogenated amorphous silicon (a-Si : H) alloy in 1969 by Chittick et al. [1]. In 1975 Spear and Le Comber [2] found that efficient doping of this material was possible, resulting in a change in the room temperature conductivity by 10 orders of magnitude. As a result of this and subsequent discoveries, a-Si : H is now used in a large number of important and varied applications, many of which are now in commercial production. Some examples are: solar cells, electrophotography, image pickup tubes, image sensors, CCDs, FET arrays, ambient sensors, LEDs, archival and random access memories, and on-chip optical waveguides [3].

Recently, research has begun to turn to the improvement of these applications, and the development of new ones, through the use of other amorphous silicon based alloys. The great potential of amorphous semiconductor alloys lies in the fact that most of their (electrical and optical) properties can be varied continuously over wide ranges by changing their composition, since stoichiometry is not required. Since lattice-matching is not needed, a wide variety of multilayer structures can be made. Low deposition temperatures allow the use of inexpensive substrates. Large-area deposition is also easily accomplished.

The purpose of this paper is to catalog the present state of research into the properties and uses of amorphous Si alloys. To accomplish this, we begin with a summary of the fabrication techniques that have been, or could be, used to produce amorphous Si alloys. The importance of this topic cannot be overemphasized; as anyone who has worked with amorphous materials knows all too well, most if not all of the physical properties of these materials are highly sensitive to the conditions under which they were made. One cannot, in general, separate the material from its method of fabrication. We then go on to describe the electrical and optical properties of all amorphous Si alloys that have been studied to the present date. Finally, we discuss the various existing and proposed applications for these interesting materials.

This review will focus on experimental results; theoretical discussions will be included only in reference to specific experimental interpretations, and only when a substantial consensus has been demonstrated. Also, we will concentrate on electrical and optical properties, as these are the main properties of interest in most amorphous silicon based applications. Thus, structural, mechanical and magnetic properties (which are the major areas of study for amorphous silicon–metal alloys, for example) are beyond the scope of this review. Throughout, we have attempted to maintain a succinct and uncluttered style, often replacing detailed discussion with pertinent references. This has allowed us to present a comprehensive and unified view, without sacrificing accuracy or readability.

1.1. Notation and conventions used

An amorphous material is one in which there is no discernible lattice periodicity. Such materials are often referred to as being vitreous, glassy or non-crystalline. The alloys will be named according to accepted convention, which is for example, a-Si : C : H for hydrogenated amorphous silicon–carbon alloys. Any other abbreviations used will be explained as they are introduced.

Amorphous semiconductors may in many cases be usefully compared on the basis of the activation energy, E_a (defined by $\sigma_d = \sigma_0 \exp(E_a/kT)$) and the optical energy gap, E_0 (defined by $(\alpha E)^{1/2} = E - E_0$). The standard techniques for obtaining these and other important parameters from experimental data can be found in most of the papers from which such values were quoted. We also refer the reader to the classic book by Mott and Davis [4], and to more recent books by Zallen [5] and the Institute for Amorphous Studies [6].

2. Preparation methods

There is a great variety of methods used to produce amorphous silicon alloys. The method used to produce a particular material depends primarily on two considerations:

(1) the glass-forming ability (GFA) of the alloy,

(2) the desired form of the material. Recent results on glass-forming ability have been reviewed by Zallen [5], Davies [7] and Pavuna et al. [8], though it should be mentioned that a deep eutectic in the equilibrium phase diagram generally indicates easy glass formation. The success of a particular deposition method depends on the cooling rate that can be obtained. The higher the cooling rate, the more alloy systems can be prepared, and the wider the composition range possible in each system (for compositions centered about the eutectic(s)). A brief review of preparation methods has been given by Lieberman [9]. These and other results will be presented in the following subsections.

Most preparation techniques are variations of a few basic schemes. Since even a moderately detailed treatment of amorphous material production processes would fill a fair-sized monograph, we will discuss only the basic processes, referring the reader to more complete sources of information.

Fabrication methods for amorphous materials can be classified according to the underlying physical principles used:

(1) production by quenching from the molten phase (rapid quenching),

(2) deposition by "atomization" (evaporation, sputtering),

(3) deposition by chemical processes (CVD, glow-discharge),

(4) surface or bulk amorphisation.

2.1. Production by quenching

These processes utilize the formation and subsequent quenching of a melt of the desired composition into an amorphous solid material. The melt is

formed by one or more of the usual heating methods: resistive, electron-beam, laser, induction or plasma jet. If the melt is quenched through contact with some external cooling medium, the material will be produced in a bulk (or powder) form. If the bulk of the solid is used to cool a melted region, then the amorphous material will be in the form of a modified surface layer. Both these processes are discussed in this section.

Amorphous materials produced in bulk form are often referred to as glasses; the two main groups being the chalcogenide glasses and glassy metals. All bulk amorphous materials are made by some form of quenching of the melt. In these processes a liquid melt of the desired composition is formed, and then rapidly cooled so that nucleation and crystallization do not have a chance to occur. Bulk quenching methods are limited to cooling rates of less than 10^7 K/s; so the kinds of amorphous materials that can be produced in this form are limited to a very few pure elements, alloys containing high concentrations of metallic elements (transition and noble metals), and the chalcogenides. One other general feature of quenching processes that should be noted is that the higher the cooling rate of a given process, the smaller the quantity of material that can be produced by that process [9].

The highest cooling rates of any fabrication process (excluding ion implantation) are found in pulsed energy quenching processes. These techniques have typical cooling rates of 10^{10} K/s. However, such processes are limited to producing thin surface layers of amorphous solid, supported by a much larger bulk region (which was used as the cooling medium) [10].

2.1.1. Sealed-melt quenching

Normal quenching methods generally do not have the fast cooling rated needed to produce amorphous materials. However, alloys made from column 6a elements (see table 1 on page 200) are often easily formed into glasses, and can be produced in large quantities by a (relatively) slow quenching process, which we will refer to as sealed-melt quenching.

Sealed-melt quenching was first used to produce a-Si alloys by Hilton et al. in 1966 [11]. In this process, high-purity elements are sealed in an evacuated quartz vial (in amounts proportional to the desired alloy composition), which is then heated at high temperature (1000 °C) in a rocking furnace for long periods (16–40 h). The vial is then quenched to room temperature in air or water. This process is capable of producing tens of grams of glassy material in a single run [11]. However, this process has a very low cooling rate, and thus is only capable of producing glasses of a limited type.

2.1.2. Rapid quenching

Rapid quenching processes all operate on the principle of increasing the cooling rate by changing the shape of the melt in order to maximize the contact area between the melt and a cooling medium [9]. A great variety of techniques have been developed to implement this process. Lieberman [9] has given a brief review (containing a thorough bibliography) of the commonly used techniques.

Rapid quenching methods can be classified according to whether they are one-shot or continuous processes. One-shot techniques produce material in the form of small foils, while continuous process produce filaments or ribbons. One-shot processes are referred to generically as "splat" quenching, while continuous processes are usually some form of "melt-spinning" technique.

Rapid quenching processes were pioneered by Pol Duwez and co-workers in 1960 [12]. They produced the first metallic glass (a-Si : Au) by a form of splat quenching known as the gun technique. This method uses a shock-tube to propel the molten alloy onto a thermally conductive substrate at high velocity. This has probably the highest cooling rate of all the rapid quenching processes, perhaps as much as 10^8 K/s [13].

A wide range of variations of this theme have been used by other researchers [9]. Only the basic types will be mentioned here. Piston-and-anvil and twin piston methods squeeze a falling melt between colliding cooling surfaces. Arc-hammer techniques use an arc or plasma jet to produce a melt on a flat, water-cooled hearth, which is then flattened by striking with a hammer. A somewhat different method, referred to as melt spraying involves spraying the melt through a plasma flame, which breaks the melt up into droplets which then condense on a substrate. All these processes have cooling rates in the range of 10^6 to 10^7 K/s.

Splat quenching techniques suffer from some serious limitations, despite their relatively high cooling rates. The quantity of material produced is very small, and is produced in a very irregularly shaped form (especially in thickness), which makes these materials unsuitable for many mechanical and electrical studies [9].

Considerable effort has gone into the development of new fabrication techniques designed to overcome the limitations of splat quenching processes. A major breakthrough was the invention by Pond and Maddin [14] of a continuous ribbon-forming process. This development allowed large scale manufacture of glassy metals, and also made available large quantities of material in forms suitable for the study of their electrical, optical, magnetic, mechanical and chemical properties.

The most common form of rapidly quenched alloys is that of ribbons a few mm wide and on the order of tens of microns thick. These continuous ribbons are made by some form of "melt spinning" [8,9]. These processes involve ejecting the molten alloy onto a thermally conductive spinning surface so that a continuous stream of molten material is rapidly quenched. There have been a number of techniques developed to accomplish this. Helical ribbons are produced by injecting the melt onto a spinning disc or drum. The latter method can also be used to produce filamentary material. Straight ribbons can be made using single or twin rollers or rapidly moving belts. These processes have cooling rates on the order of 10^6 K/s.

It is often desirable to have samples in the form of wires or filaments, and several techniques have been developed to produce such samples [9]. The most common methods inject a thin stream of molten material into a gaseous or

liquid cooling medium. One of the oldest methods involves rapidly pulling a glass tube containing the melt into a thin fiber.

Large amounts of material for use in X-ray diffraction, electrical measurements, or for compaction forming into otherwise unproducible shapes can be obtained in powder form by a variety of techniques. These techniques will not be discussed in this paper. The interested reader is referred to the recent review by Miller [15].

2.1.3. Formation of melted surface layers

Recently, through the use of directed energy beams (lasers, electron beams), it has become possible to produce thin surface layers of amorphous materials by a new form of rapid quenching process. So far, mainly lasers have been used in these processes, and so these techniques are usually referred to as *laser quenching*. However, pulsed electron beams have also been shown to be viable [16]. A detailed review of this subject has been given by von Allmen [10].

Laser quenching processes differ from the previously discussed mechanical forms of rapid quenching in two important respects: the material quenched is much thinner, and the melt is cooled through conduction into the bulk. These differences, if properly exploited, can give cooling rates of 10^3 times that obtainable in mechanical quenching processes [10].

Laser quenching techniques can be classified according to whether they use a pulsed or continuous source. Continuous, fast scanning beams possess a number of advantages such as high throughput, capability of pattern generation, and use on preformed parts. However, presently available equipment does not appear to be capable of producing cooling rates exceeding those of splat quenching [10].

Pulsed laser quenching techniques have shown the most promise for amorphous alloy formation. Typically, a Nd : YAG laser (operating in the IR region) is used with pulse durations in the ns range, with a corresponding energy on the order of 1 J/cm^2. Such devices are capable of producing cooling rates in excess of 10^{10} K/s. However, this method is sensitive to a wide variety of parameters, including the duration, intensity and wavelength (determined by the target reflectivity) of the pulse used [10]. This technique has been successfully applied to a number of different target types. Amorphous layers have been produced by "skin melting" single and polycrystalline samples of both alloys and pure elements. A-Si : Al [17] and elemental a-Si [18] have been made in this manner. Powders, either crystalline or amorphous, can be quenched into surface layers or thin films by either pulsed or continuous techniques [10].

The most successful and versatile laser quenching technique, originally developed by von Allmen [19], uses a composite target made from several very thin (15 nm) alternating layers of the desired alloy constituents in the appropriate thickness ratio. These layers are deposited using conventional techniques such as evaporation. Upon irradiation with the laser pulse, a homogeneous melt is produced which cools to form an amorphous alloy layer

several hundred nm thick. A number of amorphous silicon–metal alloys have been made using this process, over virtually their entire composition range [10].

Although a new technique, laser quenching has already demonstrated superiority over all rapid quenching and vapour deposition techniques in its ability to produce amorphous alloys. This process makes it possible to study more amorphous alloys over wider composition ranges, and could become a widely used fabrication method for the study and application of these materials.

2.2. Deposition by atomization

These processes are based on the condensation and solidification of an atomized solid into an amorphous thin film. Atomization is usually accomplished by either sputtering or evaporation. These are common methods of thin-film fabrication, and are discussed in detail in many books on thin-film technologies, such as the ones by Maissel and Glang [20] or Vossen and Kern [21].

Obviously, if a material has been atomized, then (in analogy to quenching processes) the largest possible surface area is presented to the cooling surface (substrates), and therefore very high cooling rates are possible. Evaporation and sputtering processes are generally considered to have cooling rates on the order of 10^8 K/s, though some results indicate that evaporation is superior to sputtering in this regard. To ensure that the films are deposited in an amorphous form, the substrate temperature must be selected to remain well below the crystallization temperature of the alloy. For amorphous Si, this usually means below 300 °C. For an amorphous alloy, this may imply temperatures below room temperature. In these cases the substrates must be cooled with water or liquid nitrogen. Regardless of the temperature selected, it is vitally important when dealing with amorphous films that the substrate temperature be known and controlled.

2.2.1. Evaporation systems

It should first be pointed out that Si should always be evaporated with an electron beam for optimum film purity, because of its high melting temperature and reactivity with most resistive heating sources [22]. The most direct method of depositing an alloy by evaporation is to simply evaporate existing bulk alloy material (crystalline compounds or sintered mixtures, for example). The difficulty with this is that different vapour pressures of the alloy constituents will not allow the evaporant to evaporate congruently (notable exceptions are the Si oxides) [22]. This results in films of different composition than the evaporant material, and can also result in compositional grading. A number of other evaporation techniques have been developed to overcome the problems associated with this simple but limited deposition process.

If the elemental constituents of an alloy are both solids, then they can be evaporated simultaneously in separate sources in a popular technique known as co-evaporation [22]. In this case, complete control of the composition is possible, and optimal evaporant sources can be used for each alloy component. However, a spacial dependence in the film composition is produced. Recently, it has been found that *sequential* evaporation of thin layers of different materials can result in amorphous binary alloy formation [23]. It appears that mixing and amorphisation occur as the second layer is being deposited. Some amorphous alloy films are formed with no subsequent processing, though a-Si : Rh and a-Si : Au result after an annealing stage [23].

If some of the alloy constituents are in a gaseous form, then some form of reactive evaporation must be used [22]. In its simplest form, evaporation is carried out in an atmosphere composed of the desired gases, rather than in a vacuum. Incorporation of these gases can be enhanced by using an activated reactive evaporation (ARE) [24] technique, where a positively biased probe or grid is used to attract electrons from the electron beam and to encourage collisions with the gas molecules, ionizing them and making them more reactive [24–28]. This technique has successfully been used to produce a-Si : H [25–27] and a-Si : N : H [28]. This method can be taken to its extreme form by firing a plasma or ion beam of the desired alloy atoms at the growing films [29], a process sometimes called direct synthesis. Any one of these reactive evaporation techniques can be used in conjunction with single or multi-source evaporation processes.

The various evaporation techniques described above have all been used to fabricate a-Si based films. There are, however, other techniques that could be used, though generally they are not. These unconventional methods will now be briefly described.

A problem with using an electron beam to evaporate a material is that X-rays are emitted from the melt, which produce electricaly active defects in the film [26]. This problem can be overcome through the replacement of the electron beam with a laser beam [30]. This technique is called laser evaporation, and has been used to deposit a-Si : H using a pulsed Nd : YAG laser in a hydrogen ambient [30]. Greatly enhanced deposition rates of 10^6 Å/s were obtained [30].

Compositional variations due to single-source evaporation can also be avoided by using a flash evaporation technique, where small portions of evaporant are evaporated so rapidly that dissociation cannot occur to a significant extent. In these processes a series of small pellets (or flow of powder) is dropped onto a very hot filament or plate [22]. The composition of films produced by flash evaporation is almost always the same as the evaporant material, and excellent compositional homogeneity can be obtained [22].

There are also several more drastic evaporation methods available for the deposition of alloys. The exploding-wire technique is probably the oldest method of depositing thin films. Deposition is accomplished by exploding a conducting filament with a high-current density transient [31]. Arc evaporation

uses an arc discharge between two electrodes composed of the desired alloy constituents [31]. Such methods do not produce readily reproducible results, and would normally be used as either a last resort, or in conjunction with more reliable systems.

2.2.2. Sputtering systems

Like evaporation, sputtering is a popular and well understood method of thin film fabrication. Unlike evaporation, sputtering systems generally do not require extensive modification in order to produce alloys, and so have become the preferred method for thin-film alloy fabrication. Because amorphous alloys are produced using standard sputtering systems, we will not discuss these systems in any detail here. We will, however, classify the basic processes and mention some specific modifications that have proved to be of particular importance in the production of amorphous alloy systems. Excellent descriptions of sputtering techniques have been given by Vossen and Kern [21] and by Wehner and Anderson [32]. The application of sputtering to the production of a-Si : H has been thoroughly reviewed by Moustakas [33] and Thompson [34]. In the following paragraphs we will briefly summarize the principles behind the major sputtering techniques.

Sputtering can be performed through the use of either plasmas (glow discharges) or ion beams [21]. The plasma or ion beam is used to bombard a target with energetic atoms, which "knock off" atoms from the target. These atoms are emitted from the target onto the substrates, where a thin film forms. As in the case of evaporated films, one of the most important control parameters is the substrate temperature. We restrict our discussion here to plasma-based systems. Ion beam deposition systems are essentially similar, except that the method used to produce the beam is irrelevant.

Glow discharges used in sputtering can be supported by dc or rf electric fields, though rf sputtering is presently the most common sputtering technique used to fabricate amorphous Si alloy films. The glow discharge can be enhanced by increasing the electron population by heating the cathode (triode sputtering) [21] or by illuminating it with UV radiation [32]. To increase the ionization efficiency of existing electrons, transverse and/or longitudinal magnetic fields can be applied (magnetron sputtering) [21]. Also, if gaseous impurities are a problem, then part of the depositing film can be used as a getter (getter sputtering) [21].

In the fabrication of alloys by a sputtering technique, one can use either an alloy or compound as the target material, or a composite target. Generally, in neither case is the composition of the film the same as the targets. The first technique results in graded films as one element is preferentially sputtered away. In the second case, however, the composition of the film is directly proportional to the relative areas of the elements that make up the target. An excellent technique developed by Hanak [35] uses a split-disc target geometry to produce a film having a continuous variation in composition along its length. With this technique, the properties of an entire alloy system can be

studied from single samples, so that process variations between runs are no longer a problem. A more complicated dual-target system has been developed in order to allow optimal control of most of the deposition parameters [36].

As with evaporation systems, gaseous components can be incorporated into the films by introducing the desired gases into the glow discharge. This is referred to as reactive sputtering [21]. We make no distinction here as to whether or not the reactant gas is decomposed by the glow discharge, though such processes are sometimes referred to as sputter-assisted plasma chemical vapour deposition (SAP–CVD) [37]. Obviously, reactive sputtering can be used in combination with most other plasma sputtering systems (getter sputtering is an exception).

2.2.3. Ion beam systems

Ion beams can be used to deposit amorphous thin films in two different ways [38]:

(1) primary deposition; where the ion beam is composed of the desired film material, and is deposited at low energy directly onto the substrate,
(2) secondary deposition; where a high-energy beam of inert or reactive ions is used to deposit a film by sputtering.

A promising new primary ion-beam deposition technique uses ionized clusters of atoms rather than individual ions to make up the beam, and is called ionized-cluster beam (ICB) deposition. The application of this process to a-Si : H thin film fabrication has been discussed in detail by Yamada [39]. In an ICB system, the beam is formed by evaporation of a solid. The vapours are then ejected through a nozzle into a high vacuum, which causes the vapour to form clusters of 500–2000 atoms. These clusters are then passes through an ionization chamber, where bombardment by electrons ionizes the clusters. A strong potential then accelerates the clusters onto the substrates, where they condense to form a thin film. This technique can also be used in a low pressure reactive atmosphere, as in a-Si : H production [39].

The use of an ion beam as a sputtering mechanism allows greater control over deposition conditions than is possible in plasma-based systems. However, since the basic principles are not very different from plasma sputtering, we will not discuss these techniques further. The interested reader is referred to the review by Harper [38].

An obvious advantage of ion beam (especially primary) sources is that they can be used in concert with other sources to fabricate a wide range of alloys. As an example of this, a-Si : H has been produced by a combination of the two ion-beam processes, called double ion-beam sputtering (DIBS) [40]. In this system, an Ar ion beam is used to sputter a Si target, while a H ion beam impinges directly onto the growing film. Considerable control is possible over the deposition parameters in such systems.

Ion and neutron beams can also be used to amorphise crystalline compounds or mix predeposited stacked layers. These methods, in which the

beams are not used to *deposit* materials but to modify them, will be discussed in section 2.4.

2.3. Deposition by chemical processes

There is a huge variety of fundamentally different chemical deposition processes that are in use today. We will begin by removing much of this variety by pointing out that Si, or Si-based alloys, cannot be deposited from solutions [41]. Also, equilibrium reactions cannot be used to produce amorphous alloys as they produce stoichiometric, crystalline compounds. Therefore, we will restrict consideration to the two remaining chemical deposition categories: chemical vapour deposition (CVD) and plasma deposition (glow discharge).

Both of these remaining categories have a very important limitation in common; the requirement that suitable gases are available to be decomposed into thin solid films. This restriction implies that any films deposited by these chemical techniques will always contain contaminant elements from the gases, such as H, F or CI. Though chemical processes produce the highest quality a-Si : H (and some related alloy) thin films, pure a-Si (and most alloys) cannot be produced. However, since the presence of H, F and/or CI is highly desirable (even necessary) in device quality films, this is not considered a problem at the present time. Even so, it is recommended that much greater emphasis be placed on the investigation of new gases for use in chemical deposition processes, in order to increase the very limited number of amorphous Si alloys which can presently be produced by these processes.

2.3.1. Chemical vapour deposition

The fabrication of amorphous thin films by CVD offers several advantages over other techniques; two particularly important ones are the excellent reproducibility and the absence of ion or X-ray damage in the films. However, the production of alloys is hampered somewhat by the availability of suitable gases and the high substrate temperatures that must often be used. CVD processes also have relatively low deposition rates. Much research on CVD in recent years has focussed on such considerations.

There are two main types of CVD; pyrolysis and photolysis. Pyrolytic CVD is the most common CVD process, and is discussed extensively by Kern and Ban [42]. Photolytic CVD is less common, but holds great promise for amorphous film fabrication because of the low substrate temperatures that can be used. There are also a number of CVD processes that do not rely on pyrolysis or photolysis [42]. However, these processes are usually restricted to producing stoichiometric crystals as they rely on equilibrium reactions. The interested reader is referred to the discussions by Kern and Ban [42] or Campbell [43].

Pyro-CVD utilizes the thermal decomposition of various gas species flowing through a reactor vessel into deposits on the substrates [42]. There are three

basic reactor types [44]: (1) cold wall, where only the substrates are heated in a near atmospheric pressure ambient; (2) hot wall, where the entire deposition chamber is heated in a furnace, and low pressures are used; and (3) HOMO-CVD, which is similar to (2) except that the substrates are cooled to temperatures much lower than the reactant gas.

Type (1), which is normal CVD, requires careful attention to mass transfer and surface reaction rates upon which the film quality depends [42]. This process is often referred to as heterogeneous CVD (HETEROCVD), in order to indicate that the process uses heterogeneous decomposition of the gas species, and to distinguish this technique from homogeneous CVD (discussed shortly). The application of HETEROCVD to the production of a-Si : H has been reviewed recently by Kaplan [44] and Hirose [45].

Improvements in the uniformity, structural integrity, and step coverage can be obtained through the use of low-pressure CVD (LPCVD) [42,44], which uses reactor type (2). This process is typically performed at pressures between 0.1 and 1 Torr, requires no carrier gas, and the only rate-determining step to be considered is due to surface reactions.

In the past, monosilane (SiH_4) was usually used in CVD (and glow discharge) production of a-Si : H. This gas yields a relatively low deposition rate, and requires high substrate temperatures. These high substrate temperatures prevent the use of glass and stainless steel substrates, an important drawback that has resulted in extensive efforts to lower deposition temperatures. Research into deposition with higher order silanes has been undertaken as part of this effort [46]. Disilane (Si_2H_6) has been found to produce high-quality a-Si : H thin films at substrate temperatures between 400 and 600 °C. Also, growth rates as much as 20 times that obtained with monosilane were found.

During the course of research into high order silanes, it was found that the primary depositing species was SiH_2. Therefore, processes which use higher silanes than this are heterogeneous. Such processes have high deposition rates, but the high temperatures used drives the H out of the growing a-Si : H film [47], requiring post hydrogenation to improve film quality. To avoid this, homogeneous CVD (HOMOCVD) was developed by Scott [47], where SiH_2 is the predominant gas species present. This condition is created by holding the substrates at a much lower temperature than the gas (reactor type (3)). Though the deposition rate is much less than in a heterogeneous process, a-Si : H can be deposited at substrate temperatures as low as 100 °C, with the result that the films contain as much as 30 at.% H. An excellent review of the use of HOMOCVD in the fabrication of a-Si : H thin films has recently been given by Scott [47].

It should also be mentioned that the substrates can be heated by CO_2 or Ar lasers [48], allowing spacial control of deposition.

Photo-CVD has also been studied as a method of fabricating a-Si : H and related alloy thin films. Note that this method is different from laser heating of the substrates, as the gas is directly dissociated by the optical energy in

photo-CVD systems. The chief advantage of photo-CVD technique is that it is inherently a low-temperature process, typical substrate temperatures being in the range of 100 to 300 °C [49].

Direct photo-CVD has only recently become practical, due to the use of CO_2 lasers and/or disilane gas. Silane has been directly photodissociated with a CO_2 laser [50], which is referred to as laser induced CVD (LICVD). Disilane has also been directly photodissociated using halogen and mercury lamps [51]. The CO_2 laser uses resonant coupling of its IR energy to the Si-H bond's vibrational mode to decompose the gas molecules, while UV sources use energetic photons to break their bonds. These techniques are quite new, but appear to hold much promise for the fabrication of amorphous Si alloys.

The older and more common method of photo-CVD involves the addition of Hg to the gas mixture in order to enhance absorption of the light. This process is known as mercury photosensitization and is reviewed by Aota et al. [49]. Both silane [49] and disilane [51] have been decomposed with mercury lamps using this technique. Most of the work in this area has gone into finding the optimum wavelengths to use with the various gases. Despite the fact that negligible amounts of Hg are incorporated into films produced by this technique, direct photo-CVD is the superior deposition method as it avoids the contamination of the vacuum-system produced by Hg [45]. The recent use of excimer UV lasers in direct photo-CVD show much promise in this area [52].

2.3.2. Plasma deposition

In plasma enhanced CVD (PECVD), or glow discharge, deposition systems, a plasma is used to decompose gases flowing through the reactor, causing a thin film to form on exposed surfaces. The physical properties of films grown by plasma techniques are very sensitive to the deposition and plasma parameters. Despite this and the largely empirical understanding of these processes, glow discharge (GD) deposition has emerged as the standard with which all other a-Si alloy deposition techniques are compared.

GD deposition systems may be classified according to the frequency range of the electric field used to support the plasma; dc, rf or microwave. DC–GD systems are systems in which the plasma is excited by a dc electric field. We will also consider any system operating below a few tens of kHz to also be "dc", as the ions in the plasma are fully capable of following the field oscillations [53]. RF–GD systems operate in the MHz region (13.56 MHz being most common). At these frequencies, the ions cannot react to the field oscillations, and thus the primary chemical reactions occurring in the rf plasma are initiated mainly by electrons [53]. MW–GD systems operate at frequencies above 200 MHz. In these systems the ions cannot follow the field oscillations either, and the electrons accelerated by the field can follow a full cycle without hitting any of the containing walls. Also, a number of plasma resonance and cutoff conditions can be produced at these frequencies.

DC–GD systems have been discussed by Uchida [54]; we will summarize his discussion here. DC–GD systems are generally of the flat-bed, internal

electrode type, where the plasma is generated between two parallel plate electrodes. The substrates are placed on the cathode, so this basic configuration is called cathodic glow discharge. In these systems, the growing films are subject to bombardment by positive ions, which create additional defects in the films. To solve this problem, proximity DC–GD was developed. In this system, a cathode screen is inserted a few centimeters above the substrates and the plasma supported between this screen and the anode, away from the growing film. The substrates can then be biased with respect to the screen to control the ions impinging on the film. This system has a much higher deposition rate than cathodic deposition. In some cases, cathodic and proximity systems (and their rf counterparts) are referred to as diode and triode systems, respectively.

Less common DC–GD techniques are hollow-cathode [55], multipole [54,56] and Penning [54] DC–GD. The hollow-cathode technique aims to reduce electrode–plasma interactions by moving the electrodes into side recesses to that only the positive column of the discharge is contained within the main portion of the deposition chamber [55]. RF versions of this system have also been reported [57]. In a multipole GD, the plasma is supported by electrons emitted by a hot filament and confined by a multipolar magnetic structure [54,56] . The main advantages of such a system are the low operating pressures possible. Penning GD uses two cathodes surrounded by a cylindrical anode to power the plasma. A magnetic field perpendicular to the substrates (on one or both of the cathodes) forms a dense plasma between the cathodes, reducing plasma–wall interactions [54].

Recently, the extensive body of knowledge available on toroidal plasmas (resulting from plasma fusion research) has led to the use of a similar configuration in DC–GD [58]. The system consists of a metal torus used as the anode, within which a hot tungsten filament is used to generate a plasma. A supporting dc electric field is created by biasing the filament negatively with respect to the anode. A confining dc toroidal magnetic field is also applied. This system has been used in low-pressure deposition of a-Si : H from undiluted silane [58], and has demonstrated a high degree of control over the chemical species impinging on the substrates.

RF–GD systems are usually classified according to how the electric field is coupled to the plasma; inductively or capacitively, as described by Spear and Le Comber [59] in their recent review of RF–GD a-Si : H. However, new evidence suggests that such a scheme could be misleading (as will become clear shortly), and we will adopt the classification described by Hirose [53] in his discussion of RF–GD techniques. In this case the distinction is made between tube reactors (with external electrodes) and flat-bed reactors (with internal electrodes). This system can be extended to include DC–GD and MW–GD systems as well. In the following, we will summarize the discussion presented by Hirose [53].

Tube reactors can use either capacitive or inductive coupling to excite the plasma, though it appears that in "inductive" systems the rf power is actually

capacitively coupled through the dielectric tube wall [53]. Tube systems are subject to plasma–wall interactions, limited to small sample sizes and are not easily scaled up to industrial sizes. Plasma–wall interactions can be reduced by the application of magnetic fields or by making the tube diameter much larger than the substrate holder [53]. Electromagnetic pulses have also been used to break down the plasma [60].

More versatile systems make use of the flat-bed capacitive (diode) configuration, where parallel-plate electrodes are used. The substrates can be mounted on either electrode, though films grown on the "hot" (not-grounded) plate exhibit different properties than the grounded sample, due to the bias that develops [61]. As in the case of DC–GD, a screen electrode can be used to keep the plasma off the growing films, and is referred to as a triode configuration. The great advantage of flat-bed systems is that they are easily scaled up for industrial production of large-area devices. Commercial systems currently in operation are usually of the multiple-reactor type, as exemplified by the first commercial system (at Sanyo) [62] and the newer plant at Energy Conversion Devices [63].

The ionization rate of the plasma can be increased by applying a magnetic field, the system is then in a magnetron configuration. More uniform large-area deposition may be accomplished by using vertical interdigitated electrodes [64]. Greater control over the chemical species taking part in the deposition can be produced by isolating the plasma and transporting only the desired species to the substrates [65]. This technique is called remote plasma-enhanced CVD (RPECVD), and has been used to produce a-Si : N : H and a-Si : O : H alloys [65]. The use of higher silanes has also been studied in GD systems. The results obtained with disilane and trisilane include a greatly increased deposition rate and less strain within the films, allowing the fabrication of very thick films [46].

MW–GD systems are relatively new, and have seldom been used for thin film deposition. Nevertheless, as will become clear shortly, recent results indicate that MW–GD is quite versatile and capable of producing high quality a-Si : H thin films. In order to classify MW–GD systems we will adopt the scheme described by Hirose for RF–GD systems [53]. As this field is still very new, no review has yet appeared. Also, we feel that these systems, especially MW–ECR–GD systems, in which the electrons achieve electron–cyclotron resonance (ECR), show considerable promise as versatile systems for the fabrication of amorphous materials. Therefore, we will describe the various systems that have been used in somewhat more detail than was given in our presentations of the more common and well-known techniques.

The most common MW–GD systems at present are of the tube reactor type, with excitation of the plasma performed with mw fields applied from outside. In these systems, the plasma and samples are contained within a quartz discharge tube, through which gases flow. In one system, a coaxial line configuration is used to couple the field to the plasma [66,67]. The discharge tube is inserted concentrically into a cylindrical cavity. The mw power is

guided into this cavity by a waveguide perpendicular to the axis of the cavity. This system can be used to produce amorphous thin films by sputtering [66], GD decomposition [67] or a combination of the two. A similar system uses an expanded coaxial waveguide section as the deposition chamber [68]. This system also uses external coils to produce an axial magnetic field with which ECR can be achieved.

A somewhat different system utilizes a slow-wave applicator to couple the field to the plasma, which is contained in a quartz reactor vessel [69]. This system is capable of large area production and is known as the large-volume mw plasma (LMP) system. The same group has also reported a system which uses a Surfatron to create and inject the plasma into the deposition chamber [69]. A similar system uses an internal antenna to radiate microwaves into the discharge chamber [70]. These systems all require large amounts of power (on the order of 100 W). All have been used to fabricate a-Si : H thin films.

From previous discussions, it should be clear that all plasma systems mentioned so far have a number of intrinsic drawbacks. The MW–GD tube reactors in particular require hundreds of watts of continuous-wave power (as opposed to tens of watts for RF–GD). Tube systems in general have problems with impurity incorporation and damage due to plasma–wall and plasma–film interactions, respectively. Flat-bed systems are subject to plasma–electrode interactions. All these systems are electromagnetically open; that is they radiate into the environment and thus need shielding. All of these problems can be solved through the use of a microwave waveguide section or resonant cavity as the reactor vessel.

The development of such a system for thin film deposition has been pioneered by Mejia et al. [71–73], who studied the use of these techniques in the fabrication of a-Si : H thin films. We summarize their results in the following.

The closed MW–GD system is configured as a 2.45 GHz short-circuited waveguide cavity, within which the plasma is created and deposition performed. The cavity is equipped with shielded quartz windows for optical measurements. The plasma is confined through the use of an axial magnetic field applied with coils surrounding the cavity. In this configuration, the plasma can be controlled in order to completely prevent contact with the walls of the cavity, eliminating impurity incorporation into the films. Further, with the application of a sufficiently large magnetic field, conditions of electron–cyclotron resonance (ECR) can be achieved. This results in dramatically different plasma behaviour and altered film properties [72–74].

There are a number of features possessed by this system that are absent in other plasma deposition systems. The system does not radiate into the environment, contamination due to plasma–wall interactions and damage to plasma–film interactions are minimized. Because of the greater energy of the electrons due to ECR pumping (which need not be done near the films) the deposition rate is higher and the operating pressure range wider than in DC– or RF–GD systems. Without ECR, the power required is on the order of that

required for RF–GD systems (10 W). With ECR the power requirements drop almost tenfold, while improving the deposition rate. The system is extremely versatile, and the properties of a-Si : H films deposited by this method can be varied over a very wide range [72–74]. Though not yet attempted, presumably the same will be true for a-Si alloy deposition as well.

A drawback of this system is that it is not easily scaled up to industrial levels, though work is proceeding in overcoming this limitation. On the other hand, the tremendous variety of properties that can be produced in a single material (in a single non-uniform deposition, if so desired) makes this technique an excellent candidate for the production of materials for research purposes, especially in the area of amorphous alloys and devices.

2.4. Amorphisation

We will refer to amorphisation as any process that creates a solid amorphous material by either modifying a crystalline compound or mixing a mixed-phase material without the use of melting. Thus, although in practice the following techniques appear to resemble laser quenching (sect. 2.1.3.), different physical processes are involved.

Ion implantation is a well understood, standard technique for incorporating dopants into silicon. In principle there is no reason to expect that this technique could not be used to produce amorphous silicon alloys. However, we were unable to find any reported use of ion implantation to incorporate an alloy element into amorphous silicon above a concentration of about 1 at.%. This is in spite of the fact that ion implantation is expected to have one of the highest cooling rates available: 10^{14} K/s [9].

High energy (> 100 keV) ion beams of inert atoms can produce amorphous materials by either disordering a surface layer on a crystal, or by mixing a stack of several thin layers of different elements (similar to laser quenching). Ion mixing has only recently been attempted, and the exact physical mechanisms behind the process remain a subject of debate. The ion-mixing of Si and Ni to produce a-Si : Ni has been studied by Hewett et al. [75], where the critical dose for mixing/amorphisation and the dependence on the number of layers was examined. Ion mixing of Si and Sn has also been studied [76]. This technique has many of the same advantages and disadvantages as laser quenching, though control of the final composition has yet to be demonstrated.

An extremely interesting new method for the amorphisation of bulk materials has recently been demonstrated on c-Mo_2Si, where fast neutron irradiation amorphised the entire bulk sample [77]. This technique could have a dramatic impact on the entire field of amorphous materials, where local or wide-area regions of bulk amorphous material may be produced at will. This technique should definitely be studied further.

Table 1
Periodic table of the elements showing, as shaded, all elements that have been used to produce binary (see text for precise definition) amorphous silicon-based alloys.

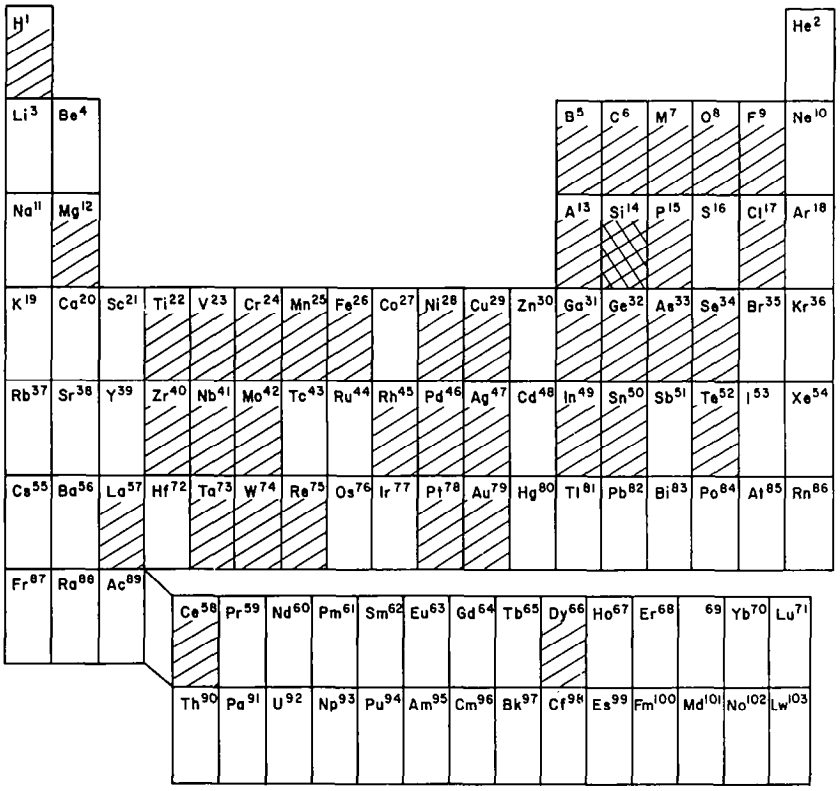

3. Electrical and optical properties

In the following sections we will describe the experimentally observed electrical and optical properties of the amorphous silicon alloys that have been studied to date. Table 1 shows all the elements that have been used in binary amorphous alloys of Si. Note that in a binary alloy we do not consider elements such as H, F or Cl, which are employed as "dangling bond terminators". For example, a-Si : Ge : H is considered to be a hydrogenated binary alloy.

We have classified the element according to the gross qualitative behaviour they produce in amorphous alloys of Si. All metallic elements are grouped together. Boron and column 5a elements (common dopants in Si) are also

taken together. Column 4a, 6a and 7a elements each make up separate groups. This system is perhaps not particularly satisfying in all respects, but does reflect genuine physical and historical divisions. Any potentially more coherent system must await the development of a stronger theoretical base for the understanding of amorphous semiconductor alloys.

3.1. Amorphous silicon–metal alloys

Amorphous silicon–metal (a-Si : M) alloys will be discussed in this section. These include all elements to the left of column 4a of the periodic table alloyed with a-Si, excluding boron and hydrogen. The a-Si : B system will be considered along with amorphous silicon alloys containing column 5a elements (covalent dopants).

No alkali (col. 1a) metals have been alloyed with a-Si, though most have been studied as dopants [78,79]. No column 2a, 2b or 3b elements have been reported either, except for a-Si : Mg (mentioned in ref. [80]). This is probably due to the high quenching rates required to form these alloys, as found from failed attempts to produce a-Si : Be by rapid quenching methods [81], though the application of more powerful techniques such as co-evaporation or laser quenching could possibly produce such alloys. A few amorphous silicon–lanthanide alloys have been made (a-Si : Ce [82], a-Si : Dy [83], a-La_3Si [84]) but have yet to be studied in any detail. No amorphous silicon–actinide alloys have yet been reported.

Most a-Si : M alloys studied are those made from noble, transition or column 3a metals. Most work on these materials has centered on new fabrication methods, critical-point behaviour (metal–insulator transition, superconductivity) and the formation of a detailed understanding of a few representative materials (a-Si : Pd, a-Si : Au, a-Si : Al). Fabrication methods were discussed earlier. The subsections on the metal–insulator transition and superconductivity portray the most active areas of study in a-Si : M alloys, since their magnetic properties (which is *the* major field of study for glassy metals) are relatively poor.

3.1.1. Basic electrical and optical properties

The first glassy metal produced was a-Si : Au made by Pol Duwez and co-workers in 1960 by splat quenching [12]. This material has become the most extensively studied of the a-Si : M alloys. The most extensively studied transition metal alloy is a-Si : Pd, also first produced by Duwez et al. by splat quenching in 1966 [85]. The first amorphous silicon–column 3a alloy studied was a-Si : Al, produced by Köster and Weiss in 1975 using electron-beam co-evaporation [86]. Many other metals have been alloyed with a-Si, though few have been studied in detail.

Through extensive study of metal–insulator transitions, it has been relatively well established that a-Si : M alloys exhibit three distinct conduction regimes with composition:

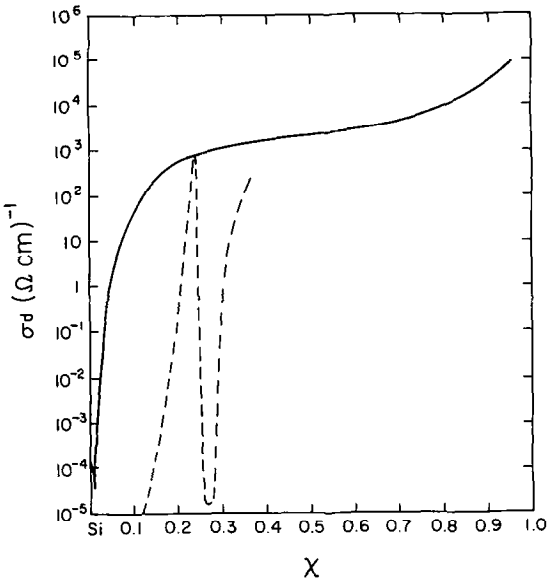

Fig. 1. Dark conductivity of a-$Si_{1-x}M_x$ alloys as a function of composition. Solid line is for M = Au, which remained amorphous for all x (from refs. [89,90]). Dashed line is for M = Al : H, in which the Al underwent microcrystallization at $x = 0.23$ (from ref. [91]).

(1) metal-doped semiconduction,
(2) mixed metallic and semi-conduction,
(3) mixed metallic conduction.

These regions are particularly well understood in the case of a-Si : Au, and are clearly seen in a graph of conductivity vs. composition, as in fig. 1. The curve for a-Si : Al : H demonstrates the behavior produced by the onset of microcrystallization of the metallic component (at about 23 at.% Al, in this case). This curve will be discussed shortly. Because a-Si : Au has been thoroughly studied, the properties of this alloy will be discussed in detail, and known similarities or differences found in other alloys described.

The electrical resistivity of a-Si : Pd for a limited range of Pd-rich compositions has been studied as a function of temperature [87], pressure [87] and hydrogen content [88]. However, there is still too little information to make significant comparisons to a-Si : Au.

The three distinct conduction regions of a-Si : Au of fig. 1 are produced by the appearance of metallic conduction in Au *and* Si at different concentrations. For Au concentrations below 14 at.%, the alloy is a semiconductor [89]. The Au atoms act as deep acceptors in a-Si, producing p-type conduction above approximately 1 at.% Au [90]. Similar behaviour has also been found in a-Si : Mn, a-Si : Ni [92], a-Si : Fe [92,93] and a-Si : Al [94], though Ta has been reported to produce n-type doping [95]. The conductivity in this region shows

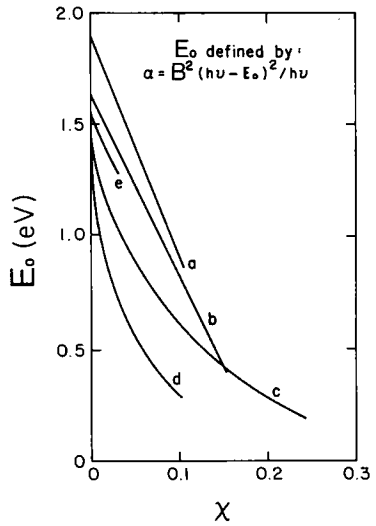

Fig. 2. Optical energy gap of a-$Si_{1-x}M_x$ alloys as a function of composition. Curve (a) is for M = Al : H, from refs. [94,96], (b) for M = Ga : H [96], (c) for M = Au [90], (d) for M = Fe, Mn, or Ni [92] and (e) for M = Ta [95].

an initial decrease (due to compensation of the intrinsically n-type a-Si), followed by a steady increase up to 14 at.% Au. Conduction is due to extended-state hole conduction above 50 K, while variable-range hopping through the Au impurity band dominates below 50 K [90]. The optical gap and activation energy show a steady decrease with increasing metal content (above ≈ 1 at.%), as shown in fig. 2. Note that the H content of the hydrogenated samples was not measured, so only gross comparisons to pure alloys can be made. Photoconductivity has also been observed in this region at low temperatures, in a-Si : Au thin films [90], but has not been reported in any other a-Si : M alloy. The extent of the semiconducting region is limited by the concentration at which the metal undergoes a transition from insulating to metallic behavior, while the Si remains semiconducting [89,90]. This transition is discussed in detail in the section on the metal–insulator transition.

In sputtered a-Si : Al : H samples the expected metal–insulator transition (at about 23 at.% Al) is masked by the onset of crystallization of the Al into isolated micro-crystallites [91]. In evaporated samples this crystallization does not occur until approximately 40 at.% Al [86]. This crystallization initially depletes the surrounding material of Al (the existing crystallites acting as nucleation centers) causing the conductivity to decrease [91]. As the crystallites grow with increasing Al concentration, a broad percolation threshold occurs, which causes the conductivity to increase again [91,97]. This behavior is also shown in fig. 1. The conductivity in this region is now a function of 3 processes: extrinsic activated hole semiconduction at high temperatures (> 300

K), metallic conduction dominated by lattice and impurity scattering at medium temperatures ($50 < T < 300$ K), and electron localization which dominates at low temperatures (< 50 K) [97]. This electron localization, indicative of two-dimensional behaviour (also producing a resistivity minimum, see below), is thought to occur in the fine metallic links between crystallites [97]. This subject has recently been the motivation for several studies of granular metal films [91]. The crystallization is the result of an insufficiently fast quenching rate, and can be obtained in many metal–insulator alloy systems.

The second conduction region extends from the metal transition to the concentration at which the Si also undergoes a transition to metallic conduction (at approximately 70 at.% Au) [89]. This transition is further described in the metal–insulator transition section. The conductivity in this region is roughly constant, as the free-electron density remains constant despite an increasing Au content [89]. Conduction in this region is independent of temperature below 50 K, but remains activated above [90]. Recently it has been found that in this region the alloy is a mixed-phase material consisting of separate domains of Au-doped a-Si and Si-doped a-Au [98]. The separate phases disappear above 45 at.% Au, and the material appears homogeneous. Presumably this is the reason for the gradually increasing conductivity in this region, the Au atoms gradually making the conduction process more metallic.

The increasing concentration of Au in the homogeneous a-Si : Au alloy eventually forces the Si atoms to adopt a disordered solid metallic (DSM) configuration above 70 at.% Au, forming the third conduction region [89,99]. Conduction is of a mixed metallic character above this concentration, and the conductivity increases as the free electron concentration approaches that of pure a-Au [89]. The unique metallic phase of Si at low pressure has been discussed by Huber and von Allmen [99]. Through comparisons with a-Au : Sn they estimated the conductivity of the DSM-Si to be approximately 10^4 $(\Omega\ \mathrm{cm})^{-1}$ [99]. Clearly this new state of a-Si requires more study.

An unusual property displayed by many amorphous metallic alloys is a resistivity minimum (as a function of temperature) at low temperatures, which also produces a negative temperature coefficient of resistance (TCR) over a wide range of temperatures and composition. Such a resistivity minimum well below a ferromagnetic transition temperature has not been observed in crystalline materials [100]. This phenomenon has been the subject of considerable study, and several theories have been proposed. No one theory has yet proven superior, and it now appears that there are several types of resistivity minima. A detailed review of the most promising theories has recently been given by Rao [100].

The resistivity minimum of a-Si : Pd has been extensively studied, and it has been concluded that the minimum in this system is due solely to the scattering of conduction electrons by trace magnetic impurities (especially Fe) [101,102]. This mechanism is known as the Kondo effect [100]. As expected, a-Si : Fe also exhibits a Kondo-type resistivity minimum, and corresponding negative TCR

[103]. The negative TCR found in a-Si : Au alloys for Au concentrations > 50 at.%) has been explained using the Ziman model [104]. In this model, extensively discussed by Mizutani [105], the resistivity of an amorphous material will exhibit a negative TCR if the following condition is satisfied [105]:

$$2k_F \approx k_P,$$

where k_F is the Fermi wave-vector, and k_P is the wave-vector corresponding to the first peak in the structure factor [100]. The Ziman-type negative TCR is more of a high temperature phenomenon than the other types, generally occurring above 30 K and is associated with a slight resistivity maximum near this temperature [105]. Resistivity minima have also been found in connection with 2-D electron localization in granular metallic films, as mentioned previously for a-Si : Al [97].

The resistivity minimum in a-Si : Zr alloys has also been studied, where a correlation between the negative TCR and superconducting properties was found [106]. Similar correlations between normal and superconducting properties have been found in a-Si : Mo alloys [107].

Finally, other a-Si : M alloys that have been made (but not studied with respect to their electrical or optical properties) are a-Si : Ti [108,109], a-Si : W (the only a-Si : M alloy made by RF–GD) [110], a-Si : Rh [111], a-Si : Re [7], a-Si : Pt and a-Si : V [10].

3.1.2. The metal–insulator transition

Mott was the first to consider the metal–insulator transition (MIT) via a reduction in the lattice constant for an ideal lattice of hydrogen atoms [112]. This led to the study of crystalline semiconductors heavily doped with shallow impurities, in which the MIT was observed with increasing impurity concentration in the hopping regime [112]. While this transition has not been observed in amorphous semiconductors doped with shallow impurities, it has been observed in several a-Si : M alloys [90]. In this case the metallic elements can be incorporated over a wide range of concentrations. MITs in general have been discussed in great detail by Mott [112], and recent interpretations reviewed by Mott and Kaveh [113]. Experimental results on MITs in a-Si : M alloys in particular have been reviewed by Morigaki [90], while more recent results can be found in a special issue of Solid State Electronics [114].

Amorphous alloy systems exhibit both compositional and topological disorder; therefore the theoretical analysis of these systems is very complicated. However, it seems clear that, except at high temperatures ($T \geq 50$ K), conduction in alloys such as a-Si : Au proceeds through hopping in the (Au) impurity band near midgap. The Mott criterion [112] for the MIT, in which N_c is the critical concentration of the metallic element, and a^* is an empirical atomic radius, is given by

$$N_c^{1/3} a^* = 0.26,$$

although there remains some dispute over the appropriate value on the right of

Table 2
Experimental critical concentrations and corresponding empirical atomic radii for a-Si : M alloys exhibiting an (assumed) Anderson-type MIT.

Alloy	N_c (at.%)	a^* (Å)	Ref.
a-Si : Al	23	1.15	91
a-Si : Au	14	1.35	90, 115
a-Si : Cr	14	1.35	116
a-Si : Fe	>16	<1.30	90
a-Si : Mn	>17	<1.27	90
a-Si : Nb	11.5	1.45	80
mc-Si : Co	15	1.33	90, 118
mc-Si : Ni	13	1.39	90, 118

this expression [90]. Table 2 shows examples of a^* estimated from the observed values of N_c for several a-Si : M alloys.

In the case of a-Si : Au and a-Si : Cr, the values of a^* from table 2 agree exactly with the empirical atomic radius of Au found by Slater [117], but the values for Mn and Fe are somewhat low. This is presumably because of hybridization of the outer 3d, 4s and 4p orbitals which further localizes the valence electrons in alloys of these transition metal elements [90].

It has been reasonably well established, particularly for the a-Si : Au system, that the MIT is an Anderson transition [112]. Further confirmation of this behavior comes from measurements of thermoelectric power, photoconductivity, magnetoresistance, electron-spin resonance and spin-dependent conductivity [90]. Collver, though working with Si : Co and Si : Ni in a metastable crystalline state, also found an Anderson-type MIT [118], His values of a^* of 1.33 (Co) and 1.39 (Ni) are in good agreement with Slater [117].

More recently, Bishop et al. [80] have studied the MIT in a-Si : Nb, a-Si : Al and a-Si : Mg, and have concluded that no minimum metallic conductivity existed, and that strong many-body contributions to the MIT were present. Möbius [119] has provided considerably support for this contention through a critical reanalysis of recent experimental work on MITs. He found that most results favour a continuous transition exhibiting no minimum metallic conductivity. A general phenomenological model was derived [119], and has been shown to be applicable to MITs in amorphous semiconductor–transition metal alloys, granular metal films and compensated and uncompensated heavily doped crystalline semiconductors.

A number of these alloy systems have also been studied in the metal-rich composition range, where a second MIT is observed. In this case the silicon switches from semiconduction to metallic conduction. This transition from covalent to metallic bonding of the Si atoms has been observed in a-Si : Au [89,99,104,120], a-Si : Ag, a-Si : Cu [120] (all at about 70 at.% metal content) and a-Si : Mo (at 37 at.% Mo) [107]. It is thought that the high concentration of metal atoms stabilizes the natural metallic state of liquid Si in the amorphous phase [120].

Another type of MIT has been observed in a-Si : Al alloys. In this system, the aluminum can be incorporated as granular crystallites embedded in a matrix of a-Si (for large Al concentrations) [91] by using quenching rates slow enough to allow partial crystallization to occur. Conduction switches from semiconducting to metallic with increasing Al content at approximately 50 at.% Al. This corresponds to a weak percolation threshold for the crystallites [91,97].

A potentially promising new material for the study of MITs is the ternary alloy a-Si : Ge : B [121]. In this case the special extent of the localized states in the gap can be increased directly through the addition of Ge [121]. This phenomenon is discussed further in sect. 3.6.

While appropriate theoretical descriptions of the various MITs in a-Si : M alloys are far from settled, one conclusion is clear: that unlike the case of energetically shallow impurities such as B or P in a-Si, the presence of metallic elements in large concentrations ($\geqslant 10$ at.%) gives rise to a wealth of interesting transport properties involving critical behaviour. For example, many of these amorphous alloys also exhibit superconducting behaviour.

3.1.3. Superconductivity

Superconducting behaviour in amorphous materials was first discovered in evaporated Bi and Ga films by Buckel and Hilsch in 1954 [122]. All amorphous superconductors exhibit type II superconductivity in the dirty limit (where the electron mean free path is much less than the superconducting coherence length) [106]. A detailed review of the latest theoretical aspects has been given by Poon [123]. In amorphous alloys, superconducting properties are exhibited over a range of compositions, through which parameters such as the critical temperature (T_c), magnetic field, and current density vary continuously.

There are two particularly interesting general results on amorphous superconductors that have arisen from previous work:

(1) The coupling between electrons and phonons in a solid is enhanced by the disorder in amorphous materials. This leads to an enhanced probability of superconductivity, and a tendency towards strong-coupling behaviour [123].

(2) The amorphous phase of a metallic superconductor is stabilized through alloying, especially with metalloids such as Si. This leads to a large increase in T_c towards the maximum predicted for the metal [123]. This is particularly true for Al, where T_c increases from about 1 K to 8 K upon ion implantation with Si [123].

For a-Si : M alloys in particular, there are four important points to note:

(1) Superconductivity has been shown to be unaffected by long-range order through studies of the Si : Pd : (H,D) [124] and Si : Zr ($T_{cmax} \approx 5$ [125]) systems [106], where it appears that only the short-range order is important.

(2) Although amorphous materials possess a lower T_c than their crystalline counterparts, they may have *sharper* transitions, as in the case of a-Si : Pd : H ($T_{cmax} \approx 3$ K). This is due to the greater overall homogeneity of the disordered phase [124].

(3) Some systems which are not normally superconductive can be made so through hydrogenation or deuteration, as in the Si : Pd system [88]. Hydrogen (and Si to a lesser extent) is thought to suppress spin fluctuations in Pd which normally prevent superconductivity from occurring [124].

(4) In the section on the MIT, it was mentioned that the presence of large metal concentrations allows the Si atoms in an amorphous alloy to form metallic bonds. This implies that it should be possible to observe superconductivity due to the Si, as has been found in amorphous germanium noble metal alloys (the noble metals Cu, Ag and Au not being superconductors) [120,126]. Superconductivity has been observed in a-Si : Au alloys ($T_c < 1$ K), but only in the range of *covalent* Si bonding [126] (the range of metallic Si bonding has not been studied at superconducting temperatures). It has been suggested that in this case the superconductivity is due to the degenerate electron system donated by the impurity (Au) atoms. If this is true, this will have been the first observation of superconductivity through an impurity band [126].

Presently, the most important application of a-Si : M superconducting alloys is in the production of ductile, high T_c materials. Applications such as Josephson junctions, superconducting magnets, motors and generators require materials with a combination of high T_c and ductility. Unfortunately, all high T_c materials are crystalline, and very brittle. Amorphous alloys are well known for their excellent strength and ductility, but have very low T_c. However, it has recently become possible to combine these two conflicting requirements through the production of the so-called A15 (or β-W) metastable crystalline compounds (T_c expected ≥ 25 K, perhaps as much as 38 K in Nb_3Si [27]) from the amorphous phase. Such production has recently been demonstrated for A15 V_3Si (a-$T_{c\max} < 1.2$ K) [128] and Nb_3Si (a-$T_{c\max} = 4.5$ K [129]) [130]. The A15 phase is very difficult to form directly [127], and is brittle in its purely crystalline form. The amorphous phase is easily formed by the usual methods, and the A15 phase is then obtained by proper annealing (under pressure in the case of Nb_3Si). A high T_c can be traded off for greater ductility by leaving some of the amorphous phase present [128].

Other superconducting a-Si : M alloy systems that have been studied are a-Si : Mo ($T_{c\max} \approx 7$ K) [107] and a-Si : Al [131].

3.2. Amorphous silicon alloyed with column 4a elements: the tetrahedral alloys

In photovoltaic solar energy conversion, the successful application of a-Si : H as a solar cell material has led to the possibility of increasing solar cell efficiency by incorporating various amounts of C, Ge or Sn into a-Si : H, thus producing tandem type solar cells (see section 4). In the following sections we discuss in detail the results obtained for amorphous alloys of Si with the column 4a elements: C, Ge and Sn. A brief review of some of the properties of a-Si : C : H, a-Si : Ge : H and a-Si : Sn : H alloy films has been published by Kuwano and Tsuda [132]. A-Si : Sn alloys are considered here because the form of tin most commonly associated with Si is the tetrahedral semiconduct-

ing form (grey or β-Sn). However, it should be pointed out that their behaviour resembles a-Si : Al and other a-Si : M alloys as much as it does the other amorphous silicon–column 4a alloys such as a-Si : Ge.

3.2.1. Amorphous silicon–carbon alloys

The great interest shown in a-Si : C : H during the past several years has mainly been due to the electroluminescent and photoluminescent properties of this material, and its successful use in improving solar cell efficiency. A-Si : C has been studied in less detail, and only in the vicinity of the 50 at.% composition range (a-SiC).

A-SiC thin films were first produced by Mogab and Kingery [133] in 1968 by rf sputtering of a polycrystalline SiC target. The electrical and optical properties of this material have since been studied by Fagen [134] and Nair and Mitra [135]. A-Si : C : H thin films were first produced by Anderson and Spear [136] by rf glow discharge in 1977. Since then, a-Si : C : H thin films have been fabricated by glow discharge in gas mixtures of silane and a hydrocarbon such as methane, ethylene or tetramethyl–silane [136–144], pyro-CVD of SiH_4/C_2H_2 mixtures [145,146], rf sputtering [137,141,147–150], PECVD [151], and by direct photolysis of pure methylsilanes or acetone and disilane mixtures [152].

In the following discussion, it is important to realize that not all researchers measured the actual C content of their films. Generally, the compositions quoted refer to gas phase or target composition ratios, which are poor measures of the actual composition of deposited films. Composition values obtained from direct measurement are given in refs. [137,138,140,149,153].

The electrical and optical properties of a-Si : C have not been studied as a function of composition; study has so far been restricted to amorphous silicon carbide, a-SiC [134–136]. As well, study of this alloy has essentially been abandoned in favour of a-Si : C : H. Therefore, we will not consider a-SiC in detail. However, it should be pointed out that conduction was found to be p-type [134], and due mainly to hopping in localized gap states even at room temperature [135,136]. The properties of a-SiC have been compared to those of a-Si : C : H, and considerable differences were found [137]. These differences appear to be a result of the presence or absence of hydrogen, and are similar to the differences between evaporated a-Si and RF GD a-Si : H [137].

The optical gap of a-Si : C : H films as a function of carbon concentration is shown in fig. 3. As the C content is increased, E_0 increases almost linearly up to a maximum at approximately 65 at.% C, before decreasing towards the value for a-C : H. It is interesting to note that in glow discharge films, increasing the deposition substrate temperature, T_s, shifts E_0 towards lower energies [137,137,144]. There are, however, some discrepancies among results from different workers regarding the actual value of E_0. These cannot be entirely accounted for in terms of differences in T_s, and point to the importance of other growth parameters, such as the H content. In sputtered a-SiC films, for example, increasing the deposition temperature has the opposite

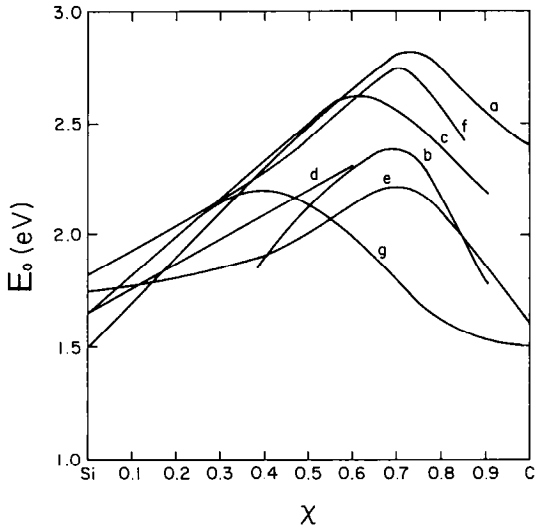

Fig. 3. Optical energy gap of a-$Si_{1-x}C_x$: H alloys as a function of composition. Curves (a-f) are for glow discharge samples, while (g) is for reactively sputtered samples. Curves (a,b) are from ref. [136], (c) from [138], (d) from [140], (e) from [142], (f) from [144], (g) from [149].

effect on E_0 [135]. The decreasing spin density accompanying this shift in the absorption edge in sputtered films strongly suggests that this behaviour results from a reduction in the density of gap states as structural defects, probably associated with multivacancies, are annealed out. In glow discharge films, ion-probe analysis showed that some H is incorporated even into high T_s films, but this does not appear to have a dominant effect on the observed shift in E_0 with T_s. Thus, for example, the optical absorption in high T_s glow discharge and in highly annealed sputtered specimens are in reasonable agreement [137].

It is worth noting that the optical gap results obtained by Tawada et al. [139] and Yamada et al. [154] are profoundly different from all other published results. In this case, it was found that E_0 increased monotonically with an increase in the methane or ethylene fraction in the gas phase. The problem in comparing these results with those of fig. 3 is that the actual C content of the films (certainly greater than the gas phase ratio [144]) was not determined. Therefore, their results were not included in fig. 3.

The refractive index of a-Si : C : H thin films varies from about 3.8 (for pure a-Si) to about 1.8 for C rich samples [138,144], as shown in fig. 4.

The effects of B doping were also studied by Tawada et al. [139] and Yamada et al. [154]. They found that B doping in a-Si : C : H thin films reduces the amount of H bonding to the C atoms (H bonding to Si is apparently unaffected) producing widening (Si rich region) or narrowing (C rich region) of the optical gap. This was also found in photo-CVD produced films [154].

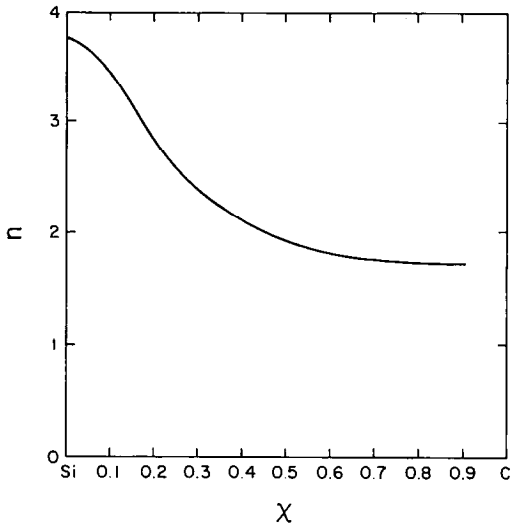

Fig. 4. Refractive index of a-$Si_{1-x}C_x$: H alloys as a function of composition. Taken from ref. [138].

It has been suggested [137] that a completely random alloy, in which one constituent is present in considerable excess of the stoichiometric composition, must contain regions in which four or five atoms of that element are bonded together. Such regions of C are more likely to bond graphitically than tetrahedrally, and their probability of occurrence can be shown to rise rapidly with increasing C content. It appears that the effect of graphitic regions is to increase the density of gap states, thus shifting the fundamental optical absorption to lower energies, as shown in fig. 3. Work on glow discharge carbon showed that as the deposition temperature was increased, E_0 decreased, implying that the structure becomes more graphitic. The change from fourfold to threefold coordination with increasing C content was found to occur at about 50 at.% C [149,155,156]. This is believed to contribute to the observed shift of E_0 to lower values in a-Si : C : H films with decreasing T_s. Graphitic bonding of the C atoms (as will become apparent in the rest of this section) appears to be responsible for much of the degradation of the electrical and optical properties of a-Si : C : H alloys. Recently, Mahan et al. [143] have observed that this type of bonding can be minimized by increasing the H incorporation in the form of CH_n ($n = 2, 3$) bonds. This has resulted in films with superior properties [143]. However, these films are still not of device quality, since polymeric bonding also degrades their electrical and optical properties [143,150]. Further improvements have been made by fluorinating the alloy [143]. The F appears to prevent polymeric or graphite C bonds from forming, improving the alloy's homogeneity and thus its optical and electronic properties [143].

Dutta et al. have studied the effects of hydrogenation [147] and fluorination [157] on the stability of a-Si : C : H thin films. They found an unexpectedly high total atomic concentration of these elements in the films, with F being the most easily incorporated (40 at.% with 6% SiF_4 in the gas phase). The effect of introducing H or F into a-Si : C : H is similar to annealing. H, and F especially, tend to bond preferentially to C over Si, with the C–F bond being very strong. This makes a-SiC : F a very thermostable material, with no deterioration exhibited up to 800 K [157]. The H concentration of a-Si : C : H increases as the C concentration increases [139,146,148,149]. Although the number of C–H bonds per C atom is larger than that of Si-H bonds per Si atom, the unpaired spin density increases from 10^{16} to 10^{20} cm^{-3} as the C content increases from 0 to 77 at.%. This increase is attributed to the change of the incorporation scheme for the H atoms, the difference in bond lengths between Si–Si and C–C, or to then tendency of the coordination number of C, to be three [141].

Photoinduced changes in a-Si : C : H have been studied by Iida and Ohki [148]. They found two types of photoinduced changes in these alloys:

(1) photobleaching; a shift in E_0 to higher energies upon exposure to bandgap illumination in the presence of oxygen.
(2) photodarkening; a shift in E_0 to lower energies upon exposure to bandgap illumination in a vacuum.

These effects were accompanied by changes in film thickness: an increase with photobleaching, and a decrease with photodarkening. These effects became more pronounced as the C content increased. It was found that photobleaching also resulted in the appearance of a C–O stretching mode in IR measurements. However, no satisfactory explanation could be found to account for both phenomena. It should be pointed out that thermal effects were ruled out by experiment, and sub-band gap illumination failed to produce any photoinduced changes.

The dc dark conductivity of a-Si : C : H thin films is due primarily to extended state conduction at and above room temperature [136,147], while hopping within localized gap states dominates below [147]. The conductivity parameters σ_d, σ_0 and E_a for the high temperature regime are shown in fig. 5. At about 80 at.% C, there occurs a precipitous decline in E_a and σ_0, suggesting that hopping within gap states has begun to dominate conduction even at room temperature [136]. Completely different results were obtained by Bullot et al. [142], who reported two regions of extended state conduction, possessing different activation energies, above and below 350 K. No trends in E_a or σ_0 were found as a function of composition [142]. Because interest in a-Si : C : H has focussed on optical properties, little work has been done on dc conductivity, and considerable uncertainty remains about the nature of this fundamental property. We strongly suggest that studies of this easily measured parameter be included in all work on this material, at least until it is reasonably well understood.

The photoconductivity of a-Si : C : H thin films has been extensively studied [137–139,142]. Unfortunately, quantitative comparisons would be misleading,

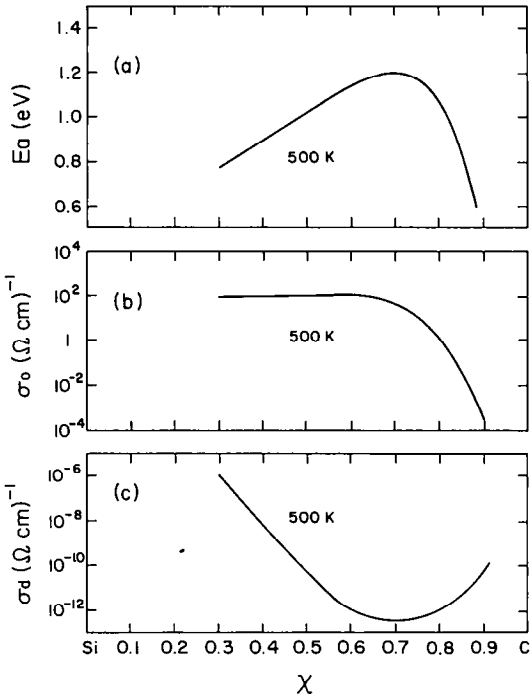

Fig. 5. Dark conductivity parameters of a-$Si_{1-x}C_x$:H alloys as a function of composition. (a) is the activation energy, (b) the pre-exponential factor and (c) the conductivity. Taken from ref. [136].

as each study has used different illumination methods. However, a number of important trends have been clearly identified. The photoconductivity is strongly dependent on composition; decreasing by between 3 to 8 orders of magnitude as the C concentration increases above 10 at.%. The consensus on this phenomenon tends to favour the worst case (8 orders) [137,138,142] rather than the best [139]. The shape of this dependence also varies between researchers. The decrease has been attributed to an increase in localized tail states, producing a decrease in the mobility–lifetime product [137,138]. Below 10 at.% C, it is possible to have the photoconductivity reach a maximum value which can be greater than that of pure a-Si:H films [137].

The decrease in σ_{ph} can be partially compensated for by B or P doping. Tawada et al. [139] found that a-Si:C:H films produced from methane (CH_4) exhibited a stronger σ_{ph} recovery with doping than did ethylene-produced (C_2H_4) films. It was also found that even undoped methane-produced films had a stronger photoconductive response than did ethylene-produced films. Because of these facts, it is suggested that methane is to be preferred over

ethylene in glow discharge fabrication of a-Si : C : H for optical applications [139].

The energy dependence of σ_{ph} has also been studied [137,142]. As would be expected, the maximum value of σ_{ph} shifted towards higher energies, following E_0, with increasing C content [142]. More interesting, however, is a shoulder in the energy dependence of σ_{ph} at 1.2 eV (below the peak value), indicative of a local maximum in the density of states [137]. The strength of the photoconductive response was found to be directly related to the height and intensity of the corresponding 1.2 eV peak found in photoluminescence measurements [137]. Indeed, the existence of the peak (or shoulder) appears to be a necessary condition for the existence of photoconductivity in these films [137].

The photoluminescence (PL) properties of a-Si : C : H were first studied by Engeman et al. [153], whose results stimulated some controversy in this area. They found two distinct peaks, and attributed these to emissions from separate Si and C clusters [153]. Later researchers [138,140,158] found only one peak (albeit usually with some structure) which shifted to higher energies with increasing C content. This was found to be satisfactorily explained as being due to the greater disorder in C rich films extending the range of localized states into the gap [138,140,158]. However, through the use of peak deconvolution techniques, other researchers have pulled peaks similar to those seen by Engeman out of single asymmetric peaks [137]. Thus it appears that this controversy has yet to be brought to a satisfactory conclusion. Nonetheless, the fact that PL in a-Si : C : H can be efficiently produced at room temperature, and can also be made to appear "white" [159] means that this area will continue to remain active for some time yet, especially in conjunction with studies on electroluminescence.

A promising and possibly unique (among a-Si alloys) property of a-Si : C is visible, room-temperature electroluminescence (EL), first observed in a-SiC by Hartman et al. in 1968 [145]. They found "blue-white" EL to occur in sandwich structures subjected to relatively large dc voltages (of either polarity) [145], but did not report any detailed study of this phenomenon. Recently, the possibility of creating large-area EL display devices has motivated some detailed studies into ac EL in a-Si : C : H thin films [159,160]. In both cases, ac EL was produced in Y_2O_3/a-Si : C : H/Y_2O_3 structures. These devices use C rich materials, and produce "blue-white" [159] or "orange-white" [160] EL at room temperature. The voltage and frequency behaviours were found to be quite similar to those of conventional ZnS : Mn cells, and due to similar causes [159,160]. However, a-Si : C : H devices have higher threshold voltages ($3–5 \times 10^6$ V/cm) [159,160]. Considering the early stage of research in this area, the results are quite encouraging.

3.2.2. Amorphous silicon–germanium alloys

A-Si : Ge : H alloy films have been fabricated by rf glow discharge decomposition of SiH_4/GeH_4 [161–174], and SiF_4/GeF_4 [175,176] mixtures by dc sputtering in a triode system [177], rf sputtering [178–180], reactive sputtering

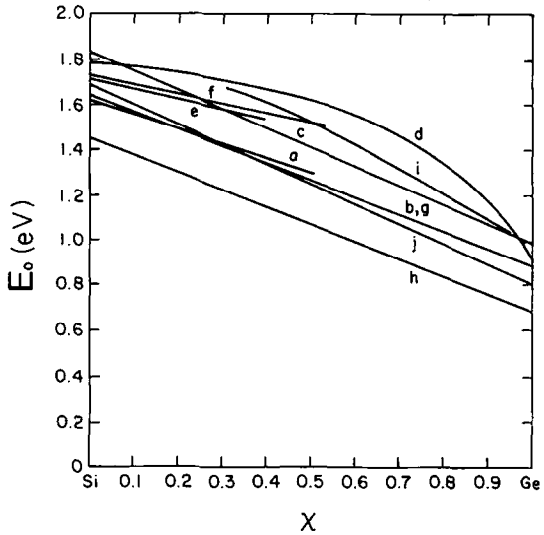

Fig. 6. Optical energy gap of a-$Si_{1-x}Ge_x$: H alloys as a function of composition. Curves (a–g) are for glow discharge samples and curves (h–j) for reactivity sputtered samples. (j) shows the dependence of the mobility gap, as derived from the dc dark conductivity activation energy [177]. Curve (a) is from ref. [161], (b) from [162], (c) from [164], (d) from [165], (e) from [167], (f) from [168], (g) from [170], (h) from [179] and (i) from [181].

[181], dual magnetron sputtering [36] and Hg-sensitized photo-CVD [182]; a-Si : Ge alloys have been fabricated by co-evaporation [183].

The optical gap of a-Si : Ge : H films decreases smoothly with increasing Ge concentration, as shown in fig. 6. Note that von Roedern [165] obtained a nonlinear trend, while the remaining researchers found a linear dependence of E_0 on composition. This difference is attributable to concurrent changes in the H content with changing Ge content. The results obtained by von Roedern were found to be a result of a rapid decrease in the H concentration as the Ge content increased above 60 at.% [165]. However, the relatively small change in E_0 at lower Ge concentrations, where the H content is constant, remains unexplained. Other researchers made no attempts to distinguish the effects of alloying with Ge or H. However, since the quoted gaps are, for all compositions, smaller than von Roedern's results, it is inferred that the H content was also smaller and the energy gap less susceptible to variations in the H concentration. One should note that the total change in E_0 in all cases is about 0.8 eV. It should also be noted that the films produced by reactive sputtering [181] have comparable, or larger, optical gaps than RF–GD produced material, which implies that the reactive sputtering method can be as, or more, efficient than RF–GD in incorporating H into a-Si : Ge : H thin films.

The variation of E_0 and other parameters as a function of H content at a fixed Ge content of 50 at.% has been studied by Banerjee et al. [178]. It was found that, with increasing H content, the absorption edge exhibited an initial blue shift, followed by a small red shift at high concentrations. This result is consistent with conductivity data which shows a corresponding minimum in the dark conductivity, and a maximum in the mobility gap. It was also found that the density of states at the Fermi level varied considerably with changes in H content; $10^{25}\ eV^{-1}\ cm^{-3}$ for low H concentrations, approaching a more reasonable $10^{18}\ eV^{-3}$ at the concentration corresponding to the conductivity minimum [178].

The optical constants of a-Si : Ge : H films, such as the refractive index, extinction coefficient and loss factor have been measured as a function of composition by Kao et al. [179], and ere found to vary approximately linearly with composition. The refractive index and extinction coefficient are dispersive and exhibit two peaks in their spectra; one above and one below the optical absorption edge. The first peak has been attributed to interband transitions and the second to transitions involving localized states in the mobility gap [179].

The spectral dependence of the optical absorption coefficient, α, has been studied by several researchers, and is shown in fig. 7. It is remarkable to see that the same feature in the density of localized states, at the same energy as in a-Si : H, still exists in the alloy. This shoulder has been attributed to a local maximum in the density of localized states in the gap, at ≈ 0.5 eV above the valence band. The proportion of characteristic defects responsible for this behaviour increases with increasing Ge concentration. Disorder-induced effects at the band edges do not seem to be significantly enhanced, as evidenced by the small modifications of the exponential part of the absorption edge. For large Ge concentrations, however, the shift of the optical absorption shoulder by about 0.15 eV and the broadening of the exponential edge suggest a modification of the distribution of localized states at the band edges. In such concentrated alloys, changes are expected in the nature of defects, introducing localized states in the lower part of the pseudo-gap. These alloys are also probably more disordered.

Conduction in a-Si : Ge is n-type over the entire composition range. Increasing Ge concentrations in the Si rich region moves the Fermi level first towards midgap, and then, in the Ge rich region, moves it back toward the conduction band [178]. Dark conductivity measurements as a function of temperature showed that the conductivity is singly-activated over a wide temperature range (room temperature to 500 K) [164,165,177]. This behaviour is attributed to extended state conduction. The room temperature σ_d increases monotonically with increasing Ge content, not only due to a decreasing activation energy, but also due to the variation of the pre-exponential factor, σ_0. While the activation energy (considered to be half the mobility gap) varies linearly with the Ge concentration (dotted line in fig. 6), σ_0 varies as shown in fig. 8. The variation of room temperature conductivity σ_d, activation energy E_0 and σ_0 are shown

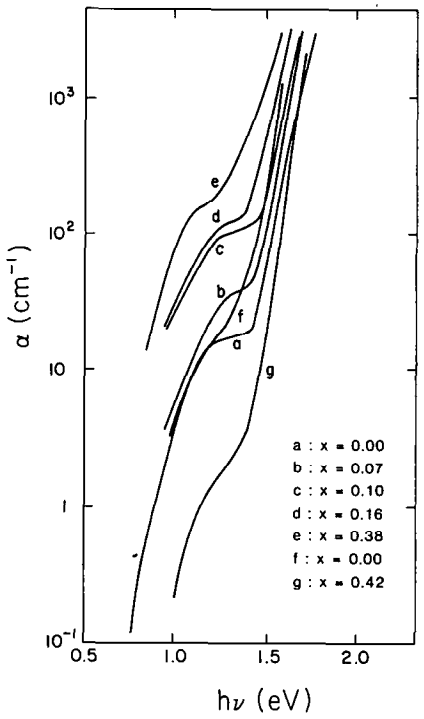

Fig. 7. Optical absorption edge of a-$Si_{1-x}Ge_x$:H alloys as a function of composition, as derived from photoconductivity measurements. Curves (a–e) are taken from ref. [167] while (f) and (g) are from ref. [165].

in fig. 8. The average value of σ_0 is about an order of magnitude smaller than that for a-Si:H. The-low temperature conductivity is consistent with a hopping mechanism between states near the Fermi level.

The photoconductivity in a-Si:Ge alloys is the subject of some debate. There are significant discrepancies in experimental results, which have also led to difficulties in the interpretation of these results. In the following discussion we will concentrate on the qualitative similarities, but will also describe the differences, which seem to arise from differences in the fabrication methods used.

At a Ge concentration of 30 at.%, the photoconductivity of dc sputtered a-Si:Ge:H decreases considerably as the Ge content is increased, and there occurs a transition from monomolecular to bimolecular recombination [177]. Films with Ge concentrations less than 30 at.% were found to be highly photosensitive, while slight P doping led to more than an order of magnitude change in the photoconductivity [177]. However, it has also been reported that even small amounts of Ge incorporated into a-Si:H result in a considerable

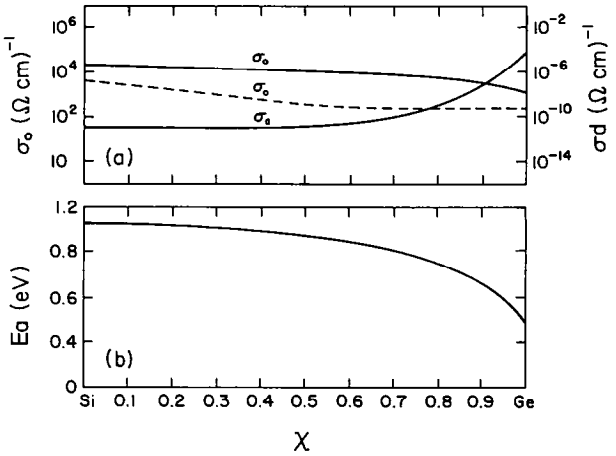

Fig. 8. Dark conductivity parameters of a-$Si_{1-x}Ge_x$: H alloys as a function of composition. (a) is the conductivity and the pre-exponential factor, while (b) is the activation energy. Solid lines are taken from ref. [165], dashed line from ref. [177].

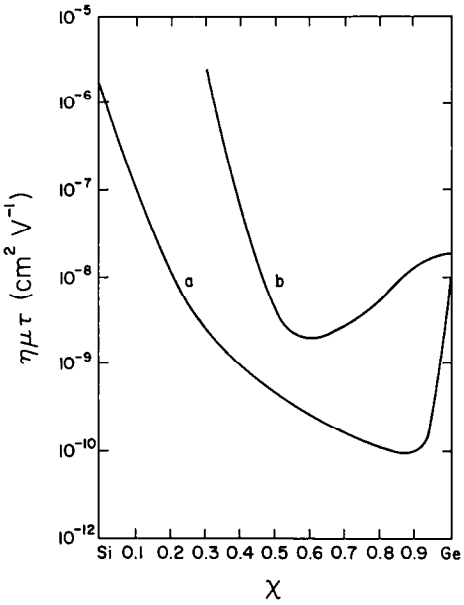

Fig. 9. Photoconductivity $\eta\mu\tau$ product of a-$Si_{1-x}Ge_x$: H alloys as a function of composition, at a temperature of 300 K. Curve (a) is taken from ref. [162], (b) from ref. [181].

reduction of the $\eta\mu\tau$ product, as can be seen in fig. 9. As may also be observed, this reduction appears to be dependent on the fabrication method used ([162] is RF–GD, [181] reactive sputtering). In this case, the degradation of the photoconductive response has been attributed to the incorporation of structural defects [162] or the increase in the number of dangling bonds on the Ge atoms [165,171]. The latter problem is thought to be enhanced by the preferential bonding of H to Si over Ge [171,181]. The decrease in the photoconductivity may instead be due to the movement of the Fermi level towards midgap as the Ge content increases in the Si rich region. This would also be consistent with the observation that the photoconductivity increases again for increasing Ge concentrations in the Ge rich region, which is accompanied by a shift in the Fermi level back toward the conduction band [162]. The photoresponse has been found to decrease initially by 3 orders of magnitude, then to increase by a factor of about 20 as the Ge content is increased [165].

Attempts to optimize the photoconductive response of a-Si : Ge : H has resulted in various recipes, depending on the fabrication process used. The degradation of the photoconductivity has been eliminated in RF–GD films by using high power [163], low substrate temperature [163] and low pressures [165], though optimized films have also been obtained at high temperatures, where the photoconductivity appears to reach a maximum in the range 5–15 at.% Ge [167]. Excellent result have also been obtained in magnetron-sputtered films, near a composition of 50 at.% Ge [36]. In this case it was found that the maximum photoconductivity was obtained when sufficient H was incorporated to produce a small amount of dihydride bonding on both the Si and Ge constituents [36]. The most recent results, however, appear to have reached a consensus, concluding that (as in a-Si : C : H) structural heterogeneity and preferential H bonding to one element are primarily responsible for the degraded photoelectric properties produced by alloying [173,174,180]. In a thorough study of diode RF–GD a-Si : Ge : H, Mackenzie et al. [174] found an optimum substrate temperature for photoelectronic properties of 300 °C. This was linked to reduced heterogeneity in these films [174]. Ichimura et al. [173] found that triode RF–GD produced higher quality films than diode RF–GD, which was also attributed to decreased heterogeneity. Similar results were obtained by Rudder et al. [180] with rf magnetron sputtering, for similar reasons. In both cases, it was hypothesized that short-lived molecular complexes were not able to take part in film growth in these systems, thus preventing the appearance of polysilane or germane heterostructures while still allowing significant H bonding to both constituents to occur [173,180]. Hg-sensitized photo-CVD has also shown promise in improving the homogeneity of these alloys [182].

In sputtered films [177] it appears that above a critical Ge content of 30 at.% the band tail below E_c is gradually broadened by the addition of more Ge. This has also been found in RF–GD material [165]. This broadening has been attributed to causes other than Si–Ge mixing; such as H-induced defects

and/or micro-structural changes resulting from the particular combination of preparation parameters used, since despite the fact that the Ge–H configuration is much less likely than Si–H [171,181], there is not a corresponding high density of non-radiative recombination centers (dangling bonds) associated with Ge. This conclusion has been supported by ESR studies [172]. However, it has also been found that increasing the Ge concentration steepens the density of the tail states in RF–GD films [162].

It appears that despite differences in the detailed changes in the DOS of samples prepared by different methods, there is an overall increase in the intrinsic state density, especially in the lower half of the pseudo-gap, which leads to a decrease in the photoelectric response. In particular, a decrease in both $(\mu\tau)_n$ and $(\mu\tau)_p$ is indicated. The distribution of gap states in a-Si : Ge : H alloys in the upper half of the mobility gap was found to increase as the Ge concentration increased, and up to a Ge concentration of 30 at.%, the general shape of their distribution was found to be similar to that in a-Si : H [169]. For concentrations above 40 at.%, a hump appeared in the distribution, at about 1.2 eV above the valence band edge, and was attributed to dangling bonds associated with the Ge atoms [169].

Light-induced defects in a-Si : Ge : H and their effect on opto-electronic properties have been studied in some detail [166,168]. A relatively small Staebler–Wronski effect was observed [166,184,185], although the density of photo-induced states is on the same order of magnitude as that in a-Si : H. This has been attributed to the fact that the large DOS created by Ge dangling bonds masks the effect of light-induced defects. Thus, the Staebler–Wronski effect cannot be observed for compositions above 50 at.% Ge. The origin of these photo-induced defects is, as in the case of a-Si : H, still uncertain. Whether these changes are a surface or bulk effect remains a matter of debate.

Although the optical gap decreases with increasing Ge concentration in a-Si : Ge : H thin films as required by practical applications in the field of solar cells, a decrease of photoresponse is also found, whatever the composition. It appears that only in the Si rich composition range (0 to 10 at.% Ge) can useful alloys be found with a moderate decrease in E_0. More studies are needed to improve the electronic properties; in particular by varying the deposition parameters and by trying to compensate the dangling bonds with atoms more firmly bound to Ge. The latter approach has recently been attempted where $SiF_4/GeF_4/H_2$ gases are used instead of hydrides [175,176]. The number of dangling bonds was reduced to 8×10^{15} cm^{-3} in an a-Si : Ge : F : H film with $E_0 = 1.4$ eV [175]. F also increases the photoconductivity by an order of magnitude, while having little effect on other properties [176]. It appears that a-Si : Ge : F : H is a promising material, particularly due to the fact that the photoconductivity is almost constant as E_0 decreases (with increasing Ge content). The electron drift mobility was found to be 0.2 to 0.3 cm^2 V^{-1} sec^{-1} in a film containing 30 at.% Ge [175]. Doping was achieved by B or P incorporation, resulting in a marked change in the number of dangling bonds [175]. At the present time, however, little is known about the properties of this

new material, and more work should be initiated on this problem, including in the direction of devices.

3.2.3. Amorphous silicon–tin alloys

A-Si : Sn alloys were first prepared by Vérié et al. [186] in 1981 using a dc triode sputtering system. Non-hydrogenated a-Si : Sn alloy films have also been prepared by co-evaporation in ultra-high vacuum [187]; whereas a-Si : Sn : H films were prepared by sputter-assisted CVD (SAP–CVD) [37], glow discharge of SiH_4, H_2 and $SnCl_4$ or $Sn(CH_3)_4$ gas mixtures [188–190] reactive [191] and rf magnetron [192] sputtering.

Vergnat et al. [187] have recently investigated the structure of a-Si : Sn alloys and found that, for Sn concentrations less than 50 at.%, Sn atoms are substituted for Si atoms, and are selectively surrounded by Si atoms in almost perfect tetrahedral units forming a continuous random network. In this composition range, the alloys are amorphous and homogeneous. As the Sn content increases, small crystallites of β-Sn appear in an amorphous Si matrix. For Sn concentrations above 75 at.%, a mixture of Si and β-Sn crystallites occurs, and the amorphous phase disappears. This is probably due to an insufficient cooling rate during deposition, similar to the situation in a-Si : Al. Annealing studies by Morimoto et al. [192] have shown that a-Si : Sn : H alloys have a low crystallization temperature, a low temperature for H evolution and a low degradation temperature for photoconductivity, making it relatively unstable. Attempts to rectify this through the addition of N were successful, but resulted in a reduced photoresponse [192].

Optical absorption measurements showed that the optical gap decreases linearly with increasing Sn content, as shown in fig. 10. This variation is consistent with the increasing refractive index found with increasing Sn concentration [186].

The dark conductivity of a-Si : Sn : H alloys was found to increase exponentially as E_0 decreased [37]. These films contained oxygen, which must presumably be eliminated if films suitable for solar cells are to be obtained. Oxygen contamination was also found in sputtered a-Si : Sn : H films [191].

The incorporation of Sn into a-Si and a-Si : H changes the predominant conduction mechanism from n-type to p-type at about 5 at.% Sn [188,189,193]. This is similar to the effect of metals added to a-Si. This transition can explain the accompanying loss in photoconductivity, as well as the poor performance in solar cell device structures. Figure 11 illustrates the transport behaviour of the a-Si : Sn : H alloys as a function of E_0 [189]. The minimum in the (room temperature) dark conductivity has been attributed to a change in conduction mechanism from n-type extended state conduction to p-type hole hopping behaviour [189]. The activation energy also indicates the change of conduction mechanism to hopping via the lower E_a values. Figure 11(c) illustrates the drastic drop in photoresponse with Sn incorporation. These workers also suggested that with the addition of Sn atoms, states of indeterminate character are created above the valuence band; with sufficient Sn incorporation the

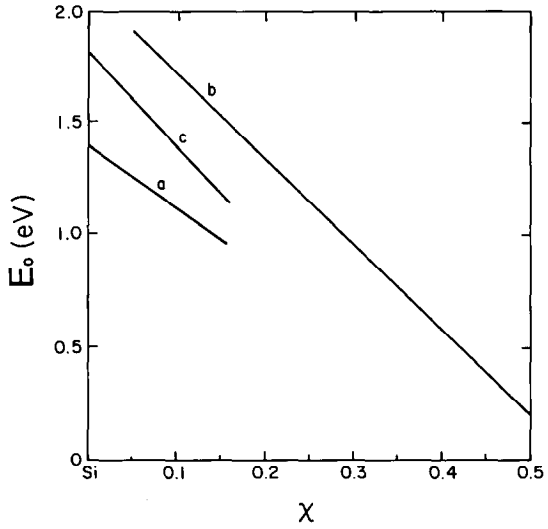

Fig. 10. Optical energy gap of a-$Si_{1-x}Sn_x$ (curve (a) [186]) and a-$Si_{1-x}Sn_x$: H (curve (b) [37] and (c) [188,189]) alloys as a function of composition.

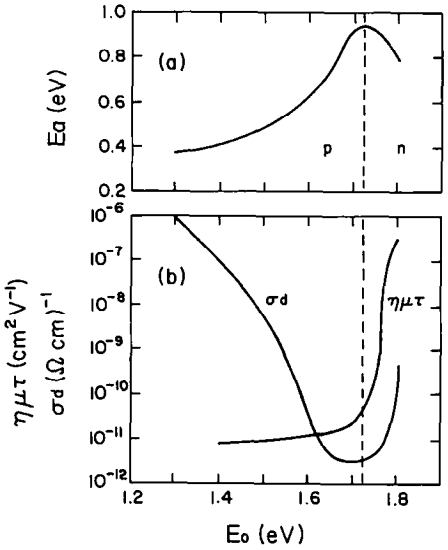

Fig. 11. Conductivity parameters of a-$Si_{1-x}Sn_x$: H alloys as a function of the optical energy gap. (a) is the activation energy and (b) the dark conductivity and photoconductivity $\eta\mu\tau$ product. Taken from ref. [189].

conduction mechanism is then changed to hole hopping within these states [189]. This interpretation was confirmed by the positive Seebeek coefficients for a-Si : Sn : H films with small E_0 (1.3 eV). Only a small percentage of the incorporated Sn atoms is deposited as impurities, producing localized states that cause the n to p-type transition. The majority of the remaining Sn atoms are incorporated substitutionally, as shown by Mössbauer results [189], and contribute to band-gap narrowing.

The conduction mechanism was found to reverse to n-type with phosphorus doping, while retaining the narrow band gap. This was accompanied by a recovery in the photoconductivity response.

3.3. Amorphous silicon alloyed with column 3a / 5a elements

3.3.1. Amorphous silicon–nitrogen alloys

Apart from a-Si : O alloys, a-Si : N alloys appear to be the most extensively studied of all amorphous silicon–nonmetal materials. We will not discuss the amorphous insulator Si_3N_4 in this review; although this material is well studied and of great technological importance in VLSI, such topics depart from the present theme of the modification of a-Si through alloying. A-Si : N : H alloys have been prepared by dc, rf and mw glow discharge in $SiH_4/NH_3/H_2$ and $SiH_4/N_2/H_2$ ambients, by sputtering in $Ar/H_2/N_2$, and by chemical vapour deposition [194–211]. Recently, application of a substrate impedance tuning method to RF–GD resulted in a high deposition rate of 22 Å/s for these alloys [198].

The presence of nitrogen has little effect on the optical gap below 40 at.% N. For larger concentrations E_0 undergoes a precipitous increase as the structure converts from a tetrahedral to a Si_3N_4 network [195,202,204]. This is shown in fig. 12.

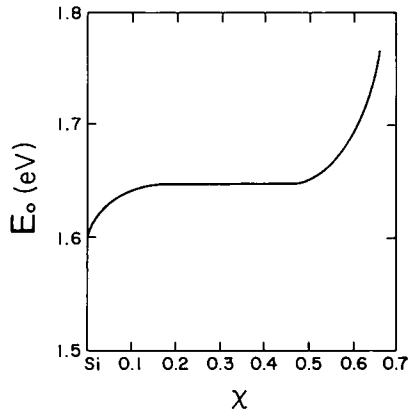

Fig. 12. Optical energy gap of a-$Si_{1-x}N_x$: H alloys as a function of composition. Taken from ref. [204].

The dark conductivity of undoped a-Si : N : H initially increases with increasing N content, followed by a dramatic decline above 40 at.%, as the optical gap increases. There is some debate as to whether N acts as a n-type dopant in small concentrations [199,200,204], though recently, Dunnet et al. [195] found additional experimental support for this contention. The mobility for electrons in the extended states has also been reported to both increase [204] and decrease [195] by as much as an order of magnitude due to N incorporation. Sasaki et al. have shown that N incorporation into a-Si : H causes an appreciable reduction in hopping conduction at the Fermi energy [210,212]. The $\eta\mu\tau$ product obtained from photoconductivity measurements is not sensitive to N incorporated in concentrations below 40 at.%, a conclusion shared by other workers [204]. N also reduces the number of ESR centers, as expected [212].

A-Si : N : H films have been doped efficiently with both boron and phosphorous; as a result of which the Fermi energy can be varied widely in the upper portion of the energy gap [200]. Boron doped a-Si : N : H exhibits a larger ratio of photo to dark conductivity than a-Si : H [201], which is of great interest in xerography and a great many other applications (see sect. 4).

Kurata and co-workers [208] have identified the stretching and bending modes of the N–H, Si–H and Si–N bonds in this material. The Si–N lattice vibrational mode corresponds to threefold coordinated N for concentrations above 20 at.% N. They believe that relatively little N is tetrahedrally coordinated, which has been supported by other workers. However, Lucovsky and Pollard [213], in reviewing the vibrational properties of a-Si alloys, point out that both N and H can bond to the same Si sites. The Si-H can also adopt a polysilane configuration. Their structural model for a-Si : N : H, for small N concentrations, includes isolated Si–H and Si–N bonding sites within a connective polysilane network [213]. More recent experimental results tend to favour Kurata's conclusions. Two thorough studies have found that there is no phase separation in RF–GD films, and that the N is randomly incorporated [195,196]. In MW–GD films, on the other hand [198], phase separation was found, even for less than 10 at.% N. Thus, as in other a-Si based alloys, the resultant structure is strongly dependent on the preparation method, and non-homogeneity is a possibility which must always be considered.

In their recent summary of tetrahedral amorphous alloys, Kuwano and Tsuda [132] concluded that the balance of published literature on a-Si : N : H alloys supports the following view:

(1) for small N concentrations, E_0 increases modestly with increasing N; the dark and photo-conductivity remain in the semiconducting range rather than the insulating range,
(2) some atoms are three-fold coordinated and some fourfold; as the N concentration increases threefold coordination becomes dominant,
(3) a-Si : N films with modest B doping, corresponding to a Fermi energy at midgap, provide optimum optoelectronic properties for a wide range of applications,

(4) the Si–H bonds in a-Si : N : H are stronger than in a-Si : H. A-Si : N : H is therefore expected to be a more thermally stable amorphous semiconductor than a-Si : H.

3.3.2. Other amorphous silicon–column 3a / 5a element alloys

This section is included for completeness, since very little work on a-Si : B, a-Si : P and a-Si : As has been published, apart from the extensive literature for doping level concentrations, which are not within the scope of this review. To our knowledge, a-Si : Sb and a-Si : Bi have not been reported in alloy concentrations. The other column 3a elements (Al, Ga, In) are metallic, and were covered in sect. 3.1.

A-Si : B : H alloys have been systematically studied by Tsai [214]. These films were prepared by RF plasma decomposition of SiH_4/B_2H_6, and covered the entire compositional range. These films also contained 10 to 40 at.% H in various bonding arrangements at both Si and B sites. Three-center bridge bonds involving B and H as well as three-center B covalent bonds give rise to a wide spectrum of bond strengths. Tail states from the conduction and valence bands penetrate deep into the energy gap. This property is exhibited in an extreme form in a-Si : B : H films deposited by low-pressure CVD, where the density of localized states is so great that no optical gap can be measured [121]. This is discussed further in sect. 3.6 on a-Si : Ge : B : H ternary alloys.

The optical gap is in the range from 1.4 to 2.0 eV; this initially decreases, and then increases again with increasing B concentration. The minimum is reached at about 40 at.% B, and the maximum at 90 at.%, as seen in fig. 13.

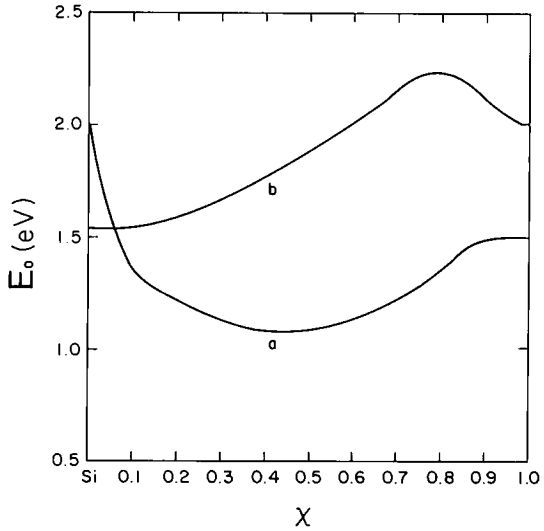

Fig. 13. Optical energy gap of $a-Si_{1-x}B_x:H$ (curve (a), from ref. [214]) and $a\text{-}Si_{1-x}As_x:H$ (curve (b) [215]) alloys as a function of composition.

A-Si : As : H alloys have been studied as an extension of As doping into alloy concentration levels in a-Si : H [215]. The optical gap of a-Si : As, shown in fig. 13, initially increases, and then decreases as the composition of the films approaches that of pure a-As : H. Over the same range the dc conductivity initially increases with increasing As content by 7 orders of magnitude (doping effect), then decreases by approximately 5 orders of magnitude with further increases in the As content. For As concentrations of 10 at.% and above, there is an As–As interaction which affects E_0 and shifts the Fermi level back towards midgap [215]. The absence of donor state formation when Si is incorporated into a-As, which should parallel the case of As incorporation into Si, remains unexplained.

A-Si : P alloys have been prepared over the full compositional range [216]. The concentration of P atoms acting as donors is a very small fraction of the total P concentration, which implies a small doping efficiency. The conductivity initially increases dramatically due to the doping effect, and the activation energy for extended state conduction decreases to 0.15 eV. With further increases in the P content, E_a increases very gradually until, at a critical concentration in excess of 90 at.% P, E_a increases rapidly by 1 eV or more. This marks the transition from a doped semiconductor to an alloy with a modified bonding structure [216].

3.4. Amorphous silicon alloyed with column 6a elements

The most widely studied alloy in this category is, of course, a-Si : O. This material is of interest for both very low O concentrations, since small amounts of oxygen are often unavoidable in a-Si : H, and for large O contents, in which the SiO_2 network is encountered. Because of the extensive literature available on SiO_x we do not include this material in our review; a brief account is bound to be misleading in its conclusions. In passing, we might point out that recent work has demonstrated that incorporated O has a generally detrimental effect on the optoelectronic properties of a-Si : H, except perhaps in extremely small concentrations (< 0.01 at.% O) [217]. To our knowledge, neither a-Si : Po or a-Si : S have been produced. The most extensively studied remaining alloy is a-Si : Te, while only little is known about a-Si : Se.

Amorphous silicon–telluride and silicon–selenide were first produced in 1966 by Hilton et al. through sealed-melt quenching [11]. A-Si : Te has also been fabricated by co-evaporation [218,219], sputtering of polycrystalline Si_2Te_3 [220], twin-roller melt quenching [221] and melt spinning in He [222]. A-Si : Se has been fabricated by evaporation of sintered SiSe [223], and by co-evaporation [223–225]. Because data on a-Si : Se is quite limited, the following discussion will focus mainly on a-Si : Te, and any similarities or disparities displayed by a-Si : Se pointed out.

Most work on a-Si : Te has been in the form of structural studies, where it has been concluded that the amorphous material consists of tetrahedral Si atoms interconnected by zig-zag chains of divalent Te atoms (the length of a

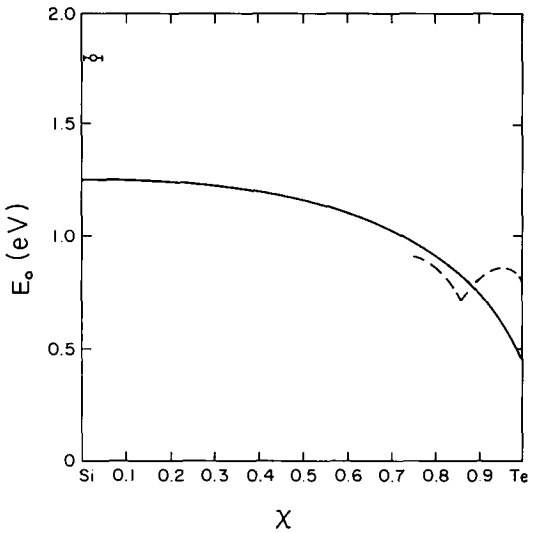

Fig. 14. Optical energy gap of a-$Si_{1-x}Te_x$ alloys as a function of composition. Also included is a-$Si_{0.95}Se_{0.05}$(0) [223]. Solid curve is taken from ref. [218], dashed curve from ref. [220].

typical chain varying directly with the Te content) [226,227]. This is a fully coordinated and stable configuration, which does not display a significant unpaired spin concentration, and does not degrade even under machining with water [220]. No structural studies of a-Si : Se have been undertaken.

A-Si : Te and a-Si : Se hydrolyze rapidly upon exposure to moist air according to the reactions [220,224]

$$SiSe_2 + 2H_2O \rightarrow SiO_2 + 2H_2Se,$$

$$Si_2Te_3 + 4H_2O \rightarrow 2SiO_2 + 2H_2Te + Te + 2H_2.$$

The occurrence of these reactions is easily discovered from the foul odour of H_2Te (or H_2Se). These reactions replace the surfaces of the alloys with SiO_2, which leads to surface and thickness effects in the electrical and optical properties of thin films of these materials [224], though bulk a-Si : Te appears to be unaffected by this reaction [220].

The optical gap of a-Si : Te decreases with increasing Te content above Te concentrations of 50 at.% Te as shown in fig. 14. The actual shape of this curve is the subject of some dispute. Peterson et al. found that E_0 is a non-monotonic function of composition [220], while we have found only a monotonic decrease [218], though such subtle features may have been destroyed by phase separation. A-Si : Se has only been studied in the range of a few at.% Se [223–225] (the exact composition was not known), so comparison with a-Si : Te is difficult. It appears, however, that even very low concentrations of Se can

raise the optical gap from 1.25 eV to 1.8 eV [223]. This has been attributed to the Se compensating dangling bonds in a manner similar to H [223]. No change in E_0 is observed in a-Si : Te below 50 at.% Te [218]. Photoconductivity (at room temperature and below) has been observed in a-Si : Te samples over a narrow composition range near that of a-$Si_{20}Te_{80}$ [218,220].

A-Si : Te is a p-type semiconductor, with an increasing conductivity with increasing Te content due to the decreasing band gap [220]. This conductivity is due to valence band conduction for temperatures down to 250 K. The activation energy for this process also appears to behave in a non-monotonic fashion [220], though only a very small composition range has been studied. The (hole) mobility is approximately 1.0 cm^2/Vs, and is temperature independent, indicating the absence of small polaron effects [220]. Also, memory-type switching has been found in Te-rich a-Si : Te materials [220,228]. A-Si : Se, for low Se concentrations, has been found to exhibit two activation energies over different temperature ranges; 0.76 eV above room temperature, and 0.41 eV below [225]. Little else is known about these materials.

3.5. Amorphous silicon alloyed with column 7a elements

Alloys such as a-Si : F(:H) and a-Si : Cl(:H) are of principal interest as alternatives to a-Si : H, in which F or Cl serve as dangling bond terminators, similar to the role played by H atoms. Their use in modifying the properties of hydrogenated a-Si based alloys has been discussed in the relevant alloy sections.

A-Si : H : F (and their use in devices) has been extensively reviewed by Madan [229], and have been shown to exhibit attractive photovoltaic properties [229,230] which are attributed to the large electronegativity of F as compared to H. This difference makes F more effective in the termination of Si dangling bonds, perhaps even by terminating more than one per F atom. The strong ionic character it introduces is also effective in reducing disorder and strain [231]. Overall, F incorporation either in place of or in addition to H, makes an a-Si based material more thermo-stable, more resistant to light-induced changes and more homogeneous. The improvement in homogeneity has proven crucial in bringing the optical and electronic properties of several a-Si based alloys up to device quality. Fluoride based gasses have the additional benefit of being safer to use.

A-Si : H : Cl alloys have been discussed by Al Dallal et al. [232]. Cl was found to be effective in the termination of dangling bonds, since, like F, its electronegativity exceeds that of H (though is less than F). Cl incorporation into a-Si based alloys has been subject to much less study than F, but is is expected to have a similar, though less pronounced, effect as F. There is, unfortunately, the possibility that Cl introduces additional states in the gap via $SiCl_2$ units [232]. F generally reduces the density of gap states as compared to H [229].

3.6. Selected ternary amorphous silicon alloys

There is a vast number of multi-component amorphous alloys which contain Si as one component. This is especially true in the case of glassy metals, where Si is often used to enhance the glass forming ability of an otherwise metallic alloy [7]. The most common of these are a-Si : Pd : X and a-Si : Fe : X alloys (where X is any one of a variety of metallic elements). In virtually all such cases the Si content is less than 20 at.%. The sheer number of these alloys precludes their inclusion in this review. This also applies to the large number of multicomponent chalcogenides which contain Si as one component. There are, however, a few ternary amorphous alloys of Si which exhibit unique properties of their own, in which Si plays a major role, and are treated as separate alloy systems in their own right. Such ternary amorphous alloy systems are considered in this section.

A-Si : Ge : B : H alloys were first produced by Murase et al. in 1982 by low-pressure CVD of $SiH_4/B_2H_6/GeH_4$ gas mixtures (diluted with He and H_2) [121]. So far, Murase et al. have been the only researchers to study this material [121,233,234]. This section summarizes their results. Though referred to as a-Si : Ge : B alloys by these authors, the large amounts of H_2 present during fabrication imply that the films contain a significant H concentration, and may be better described as a-Si : Ge : B : H alloys.

This material exhibits a number of peculiar optical and electronic properties. These properties will be discussed in this section, while other unusual properties (oxidation and Schottky contact behaviours) will be discussed in the context of their applications to microelectronics in sect. 4.

This alloy exhibits considerable optical absorption even at very low photon energies, which makes it impossible to calculate an optical gap. The conductivity of these films is also very high (≈ 0.4 $(\Omega\ \text{cm})^{-1}$). These and other measurements [121] indicate that a-Si : Ge : B alloys are characterized by a very high density of localized states distributed throughout the energy gap. In fact, the density of localized gap states is so great that conduction in these alloys, even above room temperature, is dominated by variable-range hopping through these states. This may, however, be a consequence of the fabrication process rather than the material, since although LP–CVD a-Si : B : H also has this property [121], RF–GD a-Si : B : H does not (see sect. 3.3.2.) [214].

The density of these localized gap states has been estimated at the Fermi level (pinned near the center of the gap) to be approximately 5×10^{20} cm^{-3} eV^{-1}. The nature of these gap states changes significantly with composition. Boron is incorporated into the alloy mainly in a threefold coordination, which gives the network the freedom to form a continuous random network (CRN). This CRN structure results in a very thermo-stable material. However, these threefold B atoms also produce a very *strained* amorphous network, which leads to augmented potential fluctuations that produce a high concentration of localized gap states through Anderson localization. On the other hand, the addition of Ge as a third component reduces the strain, and allows the spacial

extent of the localized-state wavefunctions to increase. This has been observed through sudden increases in the conductivity and dielectric constant with increasing Ge content. As a result, it may be possible to study a purely Anderson-type MIT at room temperature simply by increasing the Ge concentration in these films. This may have already been observed [121], but no detailed studies were undertaken. A possible complication in such a study is the tendency of Ge to induce crystallization (if presently in large concentrations), though the addition of B partially counteracts this process.

Though neither a-Si : S or a-Si : Zn binary alloys have yet been produced, a study of the ternary alloy a-Si : S : Zn : H was recently reported [235]. These films were produced by reactive rf and rf magnetron sputtering of Si and ZnS composite targets in an Ar/H_2 ambient. It was found that S was preferentially incorporated into Si-rich films, while Si-poor films consisted of approximately stoichiometric ZnS. With increasing ZnS content, E_0 increased from 1.7 eV to 3.2 eV. The addition of ZnS also reduced the spin density and photoconductivity $\eta\mu\tau$ product. It was concluded that this material is tetrahedrally coordinated in the Si-rich and Si-poor compositional regions, while a partial chalcogenide glass structure is exhibited at intermediate compositions [235].

4. Device applications

Amorphous silicon alloys have found many applications as electronic, optical and optoelectronic device materials. Many of these applications were previously exploited using the simpler a-Si : H technology, in which case the use of silicon alloys simply served to increase the efficiency of the device. An example is the improvement in the photovoltaic solar cell realized through the use of a-Si : C : H window layers and a-Si : Ge : H active layers in a-Si based devices [236]. In some cases, the use of amorphous silicon alloys has made possible applications which were not practical with a-Si : H material, thereby giving rise to new devices. An example of the latter situation is the use of a-Si : C : H in visible light-emitting diodes (LEDs), as described by Kukimoto [237].

The following subsections outline the many applications for amorphous silicon alloys which have been realized commercially, are being investigated in the research laboratory, or remain as potential device applications presently served by a-Si : H alone.

4.1. Photovoltaic solar cells

This has been the primary application of a-Si : H materials in the past, and has served as a driving force for research and development in amorphous silicon and its alloys. It should be noted that, in addition to the original application of solar cells in large-scale energy conversion, important industrial uses for these devices have been found in consumer products such as watches

and calculators. Excellent reviews are available of a-Si : H solar cells [238–243]; we confine our attention exclusively to amorphous silicon alloys and their influence on the performance of these devices.

Since photovoltaic effects were first observed in a-Si : H [244], there has been a continuous improvement in the photovoltaic efficiency from 1% in 1974 and 5.5% in 1977 (small-area devices), to the present value in excess of 11% for large-devices (1 cm^2) [238]. Even for 100 cm^2 cells, efficiencies of greater than 9% have been reported [231]. The recent advances have depended upon the incorporation of a-Si : C : H and/or a-Si : Ge : H alloys as active materials in the devices. The incorporation of a-Si : C : H as a window junction material with its increased energy gap as compared to a-Si : H, can give rise to enhanced open-circuit voltages as well as larger short-circuit currents. Both factors increase conversion efficiency. It is in a-Si : C : H/a-Si : H heterojunction cells that the best results (11.5%) have been obtained [245]. This has depended upon control of the C content of the a-Si : C : H layer [246].

The increased open-circuit voltage results from an overall increase in the diffusion potential of the heterojunction device, with its associated reduction in dark current. This is primarily due to the increased energy gap of a-Si : C : H. The short-circuit current may also be enhanced as a result of the optical absorption in a-Si : Ge : H which extends further into the infrared due to its small energy gap. This beneficial effect is difficult to exploit as a consequence of a low minority carrier lifetime in the narrow a-Si : Ge : H layer [238]. Nakano et al. [245] have recently demonstrated greatly improved properties for a-Si : Ge : H : F; in particular, photoconductivities of 3×10^{-4} $(\Omega\ \text{cm})^{-1}$ and dark conductivities of 10^{-7} $(\Omega\ \text{cm})^{-1}$. This material was made by glow discharge decomposition of $SiF_4 + GeF_4 + H_2$ gas mixtures. These advances should soon impact the efficiencies of solar cells incorporating this material as the narrow gap layer.

A-Si : C : H layers were first incorporated into solar cells by Tawada et al. [236], a-Si : Ge : H layers by Nakamura et al. [247]. The devices of Catalano et al. [248], which incorporate a-Si : C : H as a window layer in a p-i-n structure, exhibit 10.1% efficiency for 1.2 cm^2 solar cells. Nakamura et al. [249] have realized 8.6% efficient solar cells of 100 cm^2 area by using a-Si : H : Ge : H in a multilayer device.

Vérié [250] has considered the virtues of a-Si : Sn : H as the narrow gap material in solar cells. Theoretically, a 16% efficiency should be possible with an a-Si : H/a-Si : Sn : H two-cell tandem structure. Apart from the simple incorporation of low bandgap materials into a-Si based solar cells, one can effect improvements by spacially grading their alloy composition. This has been described, for example, in a-Si : Ge : H alloys by Wiedeman and Fagen [251].

The goals of the DOE/SERI amorphous silicon research project in the USA are 12% (1 cm^2) and 8% (100 cm^2) in 1986, and 13% (1 cm^2) and 12% (100 cm^2) in 1988. An additional goal of 18% (1 cm^2) for multi-junction cells has been set for 1988. This latter goal is completely dependent upon the use of

amorphous silicon alloy materials such as a-Si : Ge : H in the tandem cells [252].

It has recently been found that the light-induced degradation effects which plagued early a-Si : H solar cells can be virtually eliminated by a proper choice of silicon alloy materials and engineering of the cell structure [253]. The degradation is generally attributed to new light-induced states created in the mobility gap. By using a-Si : Ge : H : F materials in the bottom cell of a multi-junction tandem cell, efficiencies of 8–9% in very large cells remain even after prolonged exposure [231]. Clearly amorphous silicon *alloy* materials are a prerequisite to the large-scale commercialization of these solar cells.

4.2. Diodes, transistors, and other electronic devices

The electronic properties of hydrogenated amorphous silicon and its alloys are compatible with a number of active device phenomena such as fast switching in diodes and appreciable gain in transistors. Furthermore, these materials exhibit many advantages over traditional crystalline silicon in several of these applications. Among their advantages are the ability to fabricate reliable devices of large area and high power handling capability, wide operational temperature range, relative immunity to chemical and structural defects, radiation tolerance, and an enlarged range of electronic properties, particularly in the case of amorphous alloys.

Both Schottky barrier and p-i-n diodes have been manufactured with a-Si : H; these devices exhibit rectification ratios as large as 10^9 and have a very fast response [254]. The rapid response is a consequence of the small minority-carrier lifetime in the material; this response can be in the picosecond range [255]. The use of amorphous alloys provides for; (1) tailoring of the forward-bias threshold voltage due to variation of the energy gap, and (2) modification of reverse-bias breakdown voltage and response time.

A-Si : H insulated gate field-effect transistors or thin-film transistors have been investigated by many workers; see, for example refs. [254,256–258]. These devices have realized all of the advantages over crystalline devices that were cited above. The same material has also been employed in the manufacture of charge-coupled devices [259–261]. Among the many applications for the FET devices have been address circuitry for liquid-crystal display panels [262] and full-colour liquid-crystal television [263], circuitry for addressable image sensors [264,265], simple logic circuits [256] and ambient sensors [266].

Amorphous silicon alloys are alternatives to a-Si : H as the active material in these devices; since the transistor parameters derive from the carrier mobility, dielectric constants, etc., they may again be tailored to the applications. Secondary considerations such as temperature dependence and radiation tolerance will also be sensitive to alloy composition. Further improvements and fabrication ease arise from the use of silicon alloys such as a-Si : N : H as a gate dielectric, deposited in situ upon the base material of the FET device. In a FET device, incorporating layers of a-Si : H and a-Si : N : H, Le Comber [267]

has shown that the properties of a small off-current, low-voltage on-off transitions and high on/off current ratio depend upon having a low density of localized states in the materials and their interface. Field effect mobilities on the order of 0.3 $cm^2\ V^{-1}\ s^{-1}$ were obtainable in these FETs.

In addition to their purely electronic function, a-Si alloys could be used for integrated sensors, for example integrated image sensors in which both the sensor and the logic are built in the same material [268]. Various logic circuits such as inverters, NAND and NOR gates, bistable multivibrators and shift registers have been made in a-Si : H materials [269–271]. All of these applications can potentially benefit from the added degree of freedom achieved in varying the alloy composition of the substrate material. The primary drawback of logic circuits based on amorphous materials is insufficient switching speed for mainstream applications. This is not a major concern in many applications, such as those mentioned above.

Amorphous silicon-based materials have also exhibited nonvolatile memory behaviour [272–274]. The most promising structures were p-n-i arrangements with on/off resistance ratios of approximately 10^4, and switching times of less than 100 ns. This behaviour has been attributed to the formation of current filaments in the on-state [272].

Another potentially important application for amorphous silicon alloys is in hybrid diode and transistor structures with crystalline silicon. Murase et al. [243] have employed a-Si : Ge : B : H alloys in amorphous–crystalline heterojunctions. Forward threshold voltages and reverse recovery times of these diodes decrease dramatically over all-crystalline diodes. The amorphous alloy actually behaves in a similar manner to the metal contact in Schottky diodes, exhibiting high work functions equivalent to noble transition metals. Heterojunction bipolar transistors have also been made with current gains that exceed all-crystalline silicon transistors for a given Gummel number [275]. Current problems with this structure include excessive recombination at the amorphous–crystalline interface and large emitter resistance. Yet another device demonstrated recently is an a-Si : H static induction transistor [233,276], with on/off current ratios as high as 10^8. The transconductance exceeds the a-Si : H thin film transistor by a factor of approximately 400. The additional potential advantages of using silicon alloys has, for this structure, not yet been investigated.

4.3. Electrophotography, image sensors, and other optoelectronic devices

Amorphous silicon and its alloys have found many applications in electrophotography or xerography, media for laser printers, etc. These applications have recently been described by Shimizu [175,277–279]. They depend on a photoinduced discharge, which turns out to rely upon a large ratio of photoconductivity to dark conductivity in the material. Although commercial devices employing alloys have only begun to be realized, it is already known that alloys such as a-Si : N : H with $\sigma_{ph}/\sigma_d > 10^6$ [201] offer potential improvements

over a-Si : H. This was discussed in sect. 3.3.1. Similar comments apply to image pickup tubes (discussed by Ishioka [280]) and large-area image sensors (discussed by Kaneko [264]). Photodetectors and modulators with fast response times (discussed by Phelan [281]) have been fabricated in a-Si : H, and a-Si : C : H alloys have been used to produce visible LEDs [159].

Amorphous silicon alloys exhibit advantages over their crystalline counterparts, for optoelectronic applications, in the relaxation of **k** conservation rules with the attendant increase in optical absorption or luminescence efficiency. Their improvements over a-Si : H stem from the ability to extend the useful wavelength range to shorter wavelengths, as for example, with a-Si : C : H [159] or to longer wavelengths with, for example, a-Si : Ge : H [175]. These abilities apply to either photoconductive, photovoltaic or luminescent phenomena. Further advantages in stability, reliability, temperature range and other considerations are expected to accrue due to a mature fabrication technology in amorphous silicon alloy materials.

Photoreceptors for electrophotography, vidicons, solid state imagers overlaid with amorphous silicon materials, and linear line sensors for facsimile or optical character recognition are entering commercial production. The surface of a-Si : H drums in photocopiers is passivated with a-Si : C : H or a-Si : N : H [282]. Heterojunction structures such as a-Si : C : H/a-Si : H have made practical many of the imaging devices mentioned above. Highly resistive materials which retain surface charges in the imaging process employ a-Si : C : H or a-Si : N : H alloys [283,284]. To achieve the required high deposition rates for the a-Si alloys, microwave plasma deposition is presently the most promising fabrication method [72,285].

A recent study of visible injection electroluminescence in a-Si : C : H p-i-n diodes [286] has shown that compositional tailoring of the spectral response of the emitted light may be achieved at room temperature. A final example in the area of optoelectronic devices is the optically activated switches demonstrated by Wang [287]. These interesting devices are amorphous–crystalline heterojunction structures in which the amorphous layers are a-Si : H, a-Si : C : H or a-Si : N : H alloys. Transition times are in the nanosecond range.

4.4. Optical and electronic recording

The application of a-Si : H and its alloys to archival storage media, in which data is written and read by either laser beams or electron-beams, has been the topic of considerable recent study [288,289]. Information storage is accomplished by either ablative hole formation, hydrogen effusion, bubbling, or other energetically induced phenomena in the material.

In the case of electron-beam addressable material, the critical properties are the correlation of conductivity to H content or structure. In laser-addressable systems, the optical absorption, refractive index and thermal properties of the films are the important parameters. All of these features are sensitive to the alloy composition, and this nascent research area holds tremendous potential

in view of the insatiable demands of modern computer systems for extended memory.

4.5. Other applications

A host of other applications have been explored in the laboratory for a-Si : H and its alloys. These include FET ambient sensors (discussed by D'Amico and Furtunato [266]), optical waveguides [290], strain gauges [291] and various other sensors and transducers. A still more pervasive set of applications is found in microfabrication technology (discussed by Murase and Mizushima [233]), and in particular for high-resolution VLSI processing.

In the latter area of microfabrication, amorphous silicon alloys are beginning to find a variety of roles to play [233,292]. These include enhanced oxidization rates using a-Si : Ge : B : H, whose resultant oxides provide excellent passivation, self-aligned electrodes, and patterning material for directional reactive-ion etching in submicron feature definition.

A variety of other preliminary applications studied for amorphous silicon alloys are not included in this review, since it is too early to forecast their eventual commercial potential.

5. Summary and conclusions

There is a great variety of methods available for the fabrication of amorphous silicon alloys. RF–GD remains the standard to which all other techniques are compared. Presently, only this and a few other chemical techniques can be used to produce device-quality material on a large scale. Thus, to optimize the fabrication process for other alloys, effort must focus on the search for new gases to allow the production of more alloys by chemical techniques. Also, when more than one gas is available, the optimum one for a given set of material properties must be selected. Research into other fabrication systems will center on the production of materials inaccessible by glow discharge methods and the optimization of their quality. Specific advantages promised by new methods, such as high deposition rates or spacial deposition control should also be pursued. However, since the aim of much of this research is toward the production of commercial quantities of material, study of new systems should also consider how they might be scaled up to industrial levels. Two potentially revolutionary tools which remain to be exploited in alloy formation are ion beam mixing and neutron beam amorphisation.

As is evident from sect. 3, the wide range of approaches taken to the study of amorphous alloys has left the understanding of the electrical and optical properties of a-Si based alloys wanting in many basic areas. Thus, despite the surprising variety of existing a-Si alloys, the utility of many of them in solving current problems related to amorphous semiconductor devices remains to be assessed. This is particularly true of a-Si : M alloys, which may have potential

as metallization layers, or in introducing magnetic properties into otherwise normal semiconducting devices. We feel that there are several basic characterizations that would satisfy these needs and that should be included whenever possible in all studies, at least until well understood. These would be, in keeping with the nature of most potential applications: room temperature optical absorption, temperature dependence of dc conductivity and measurement of any photoconductivity that may be present. These relatively simple measurements measurements should be standard characterization procedures, as they are for a-Si : H. These results would facilitate comparison between different materials, and between similar materials produced by different research groups.

Another characterization problem, especially important in chemically-produced materials, is the need to distinguish between the effects of alloying and those of hydrogenation. This problem must be solved through direct measurement. It is now well established that the H content of an alloy does not remain constant as the composition is varied. The presence of an alloy element significantly alters the bonding environment available to the H atoms. Further, it is clear that the alloy composition is not a linear function of the gas-phase composition. Using gas-phase ratios instead of direct measurements can often be misleading.

A quite serious problem is the tendency of alloying to produce heterogeneous or phase-separated materials. Such morphologies cause a significant degradation of the electrical and optical properties of a-Si based alloys. They also make comparison between similar materials produced by different techniques difficult, especially if the morphology is not known. IR absorption and TEM measurements are very useful in this regard. These problems can usually be solved through the use of an appropriate deposition method, in concert with optimized deposition conditions. Fluorination has also proven successful in solving this problem in several covalent a-Si based alloys.

Many amorphous silicon based alloys have also been shown to be unstable upon exposure to air, heat or light. Hydrolyzation, impurity absorption, H evolution and the Staebler–Wronski effect can lead to temporal and thickness dependences in most electronic and optical properties. This can sometimes be overcome by improving the structural integrity of the material through changes in the deposition process. The degree of success that can be attained using this approach is exemplified by the great stability of sealed-melt quenched a-Si : Te as compared to vapour-deposited thin films. Thermo- and photo-stability, in covalent alloys at least, has been shown to be greatly enhanced by the use of F as a dangling bond terminator in stead of (or in addition to) H.

In a-Si : M alloys, as in the entire amorphous metal–metalloid field, there remain vast areas open to experimental study, and many fundamental questions unanswered. The existence of solid disordered metallic (DSM-Si) has only recently been discovered; its properties have yet to be studied. Of immediate interest are the possibility of superconductivity in DSM-Si and the DSM-Si to a-Si MIT. Generally, MITs in a-Si based alloys continue to be an

area of vigorous study and theoretical debate. Study of the electrical and optical properties of a-Si : M alloys has only begun; many basic properties remain to be examined. In particular, why does Ta behave as a donor in a-Si, when all other metallic elements (except alkalies) studied to date act as acceptors? How can alkali metals be incorporated to alloy concentrations in a-Si and what behaviour will result from the strong ionic component added to the bonding environment?

The chalcogenides have been extensively studied as multicomponent amorphous alloys, yet their behaviour in binary a-Si based alloys is poorly understood. A-Si : Te is the most extensively studied (outside of Si oxides) and has shown a number of interesting properties that require more investigation. Though a-Si : Se has hardly been examined at all, it has already been shown to exhibit dramatically different behaviour from a-Si : Te while the potentially most interesting alloy, a-Si : S, has yet to be produced.

In the tetrahedral a-Si alloys, understanding is now approaching a high level, and most research is now focussed toward specific applications. One of the more pressing problems is that of light-induced degradation. Solution of this problem is critical in improving the performance of tandem solar cells. A related problem is in understanding the photobleaching and photodarkening observed in a-Si : C : H.

Though H has been used with great success as a dangling bond terminator in a-Si for a decade, F has been shown to produce superior properties for a number of device applications, and may supplant H in these cases. Similarly, Cl may prove to have its own advantages in certain applications, though significant research remains to be done in this direction.

Finally, we note that tetrahedral a-Si based alloys are just now beginning to be incorporated into commercial applications such as solar cells, photocopier drums and thin-film transistors. This trend can be expected to continue at an increasing pace in a widening variety of applications, as the field of a-Si alloys matures into the mainstream of semiconductor physics and engineering.

We wish to thank Prof. K.C. Kao, Prof. R.D. McLeod, S.R. Mejia, J.J. Schellenberg, J.F. White and T.V. Herak for helpful comments. The financial support of the Natural Sciences and Engineering Research Council of Canada (NSERC operating grant A1330) is gratefully acknowledged. One of us (PKS) also acknowledges the support of a NSERC postgraduate scholarship.

References

[1] R.C. Chittick, J.H. Alexander and H.F. Sterling, J. Electrochem. Soc. 116 (1969) 77.
[2] W.E. Spear and P.G. Le Comber, Sol. St. Commun 17 (1975) 1193.
[3] J.I. Pankove, ed., Semiconductors and Semimetals, Vol. 21, Hydrogenated Amorphous Silicon, Pt.D (Academic Press, Orlando, 1984).
[4] N.F. Mott and E.A. Davis, Electronic Processes in Non-Crystalline Materials, 2nd ed. (Clarendon, Oxford, 1979).

[5] R. Zallen, The Physics of Amorphous Solids (Wiley, New York, 1983).
[6] D. Adler, B.B. Schwartz and M.C. Steele, eds., Physical Properties of Amorphous Materials (Plenum, New York, 1985).
[7] H.A. Davies, in: Amorphous Metallic Alloys, ed. F.E. Luborsky (Butterworths, London, 1983) p. 8.
[8] D. Pavuna, G. Fourcaupot and J.C. Grieco, in: Amorphous Metals and Non-Equilibrium Processes (Editions de Phys., Les Ulis, Strasbourg, 1984) p. 45.
[9] H.H. Liebermann, in ref. [7], p. 26.
[10] M. von Allmen, in: Topics in Applied Physics 53, Glassy Metals 2, eds. H. Beck and H.-J. Güntherodt (Springer, Berlin, 1983) p. 261.
[11] A.R. Hilton, C.E. Jones and M. Brau, p. 105; A.R. Hilton and C.E. Jones p. 112; A.R. Hilton, C.E. Jones, R.D. Dobrott, H.M. Klein, A.M. Bryant and T.D. George, p. 116; Phys. Chem. Glasses 7 (1966).
[12] W. Klement, R.H. Willens and P. Duwez, Nature 187 (1960) 869.
[13] P. Duwez, Trans. ASM 60 (1967) 607.
[14] R. Pond Jr. and R. Maddin, Trans. Met. Soc. AIME 245 (1969) 2475.
[15] S.A. Miller, in ref. [7], p. 506.
[16] S.T. Picraux and D.M. Follstaedt, presented at the Materials Research Society Meeting, Boston, Nov. 1982 (unpublished).
[17] G. Fuxi, S. Baorong and W. Hao, J. Non-Cryst. Solids 56 (1983) 56.
[18] R. Tsu, R.T. Hodgson, T.Y. Tan and J.E. Baglin, Phys. Rev. Lett. 42 (1979) 1356.
[19] M. Von Allmen, S.S. Lau, M. Mäenpää and B.Y. Tsaur, Appl. Phys. Lett. 36 (1980) 205.
[20] L.I. Maissel and R. Glang, eds., Handbook of Thin Film Technology (McGraw–Hill, New York, 1970).
[21] J.L. Vossen and W. Kern, eds., Thin Film Processes (Academic Press, New York, 1978).
[22] R. Glang, in ref. [20], pp. 1–3.
[23] I.E. Bolotov, A.N. Belouschchenko and V.O. Shualev, Sov. Phys.-Tech. Phys. 30 (1985) 683.
[24] R.F. Bunshah and A.C. Raghuram, J. Vac. Sci. Technol. 9 (1972) 1385.
[25] W. Pries, R.D. McLeod, T.V. Herak, S.R. Mejia, H.C. Card and K.C. Kao, MRS Proc. Symp. Poly-Micro-Crystalline and Amorphous Semiconductors, Strassbourg (1984) p. 599.
[26] G. Talukder, J.A. Cowan, D.E. Brodie and J.D. Leslie, Can. J. Phys. 62 (1984) 848.
[27] J.C. Anderson, S. Biswas, J. Non-Cryst. Solids 77/78 (1985) 817.
[28] P.K. Shufflebotham, J.F. White, H.C. Card and K.C. Kao, Appl. Phys. Lett. 49 (1986) 656.
[29] R.E. Viturro and K. Weiser, Phil. Mag. B 53 (1986) 93.
[30] M. Hanabusa and M. Suzuki, Appl. Phys. Lett. 39 (1981) 431.
[31] K.L. Chopra, Thin Film Phenomena (McGraw–Hill, New York, 1969).
[32] G.K. Wehner and G.S. Anderson, in ref. [20], p. 3–1.
[33] T.D. Moustakas, in: Semiconductors and Semimetals, Vol. 21, Hydrogenated Amorphous Silicon, Pt. A, ed. J.I. Pankove (Academic Press, New York, 1984) p. 55.
[34] M.J. Thompson, in: Topics in Applied Physics 55, Physics of Hydrogenated Amorphous Silicon I eds. J.D. Joannopoulos and G. Lucovsky (Springer, Berlin, 1984).
[35] J.J. Hanak, J. Mater. Sci. 5 (1970) 964.
[36] R.A. Rudder, J.W. Cook Jr. and G. Lucovsky, Appl. Phys. Lett. 45 (1984) 887.
[37] H. Itozaki, N. Fujita, T. Igarashi and H. Hitotsuyanagi, J. Non-Cryst. Solids 59/60 (1983) 589.
[38] J.M.E. Harper, in ref. [21], p. 175.
[39] I. Yamada, in ref. [33], p. 83.
[40] C. Coluzza, D. Della Sala, G. Fortunato, S. Scaglione and A. Frova, J. Non-Cryst. Solids 59/60 (1983) 723.
[41] F.A. Lowenheim, in ref. [21], p. 209.
[42] W. Kern and V.S. Ban, in ref. [21], p. 258.
[43] D.S. Campbell, in ref. [20], p. 5-1.
[44] D. Kaplan, in ref. [34], p. 177.
[45] M. Hirose, in ref. [33], p. 109.

[46] M. Hirose, in: Jpn. Ann. Rev. in Elect., Comp. & Telecomm. 16, Amorphous Semiconductor Technologies & Devices, ed. Y. Hamakawa (OHMSHA & North-Holland, Amsterdam, 1984) p. 67.
[47] B.A. Scott, in ref. [33], p. 123.
[48] D. Bäuerle, P. Irsigler, G. Leyendecker, H. Noll and D. Wagner, Appl. Phys. Lett. 40 (1982) 819.
[49] K. Aota, Y. Tarui and T. Saitoh, in ref. [46], p. 98.
[50] M. Meunier, J.H. Flint, D. Adler and J.S. Haggerty, J. Non-Cryst. Solids 59/60 (1983) 669.
[51] Y. Mishima, Y. Ashida and M. Hirose, J. Non-Cryst. Solids 59/60 (1983) 707.
[52] J. Gianinoni and M. Musci, J. Non-Cryst. Solids 77/78 (1985) 743.
[53] M. Hirose, in ref. [33], p. 9.
[54] Y. Uchida, in ref. [33], p. 41.
[55] S. Matsumura, K. Sakurai, A.A. Berezin, R.M. Hobson, S. Teii and J.-S. Chang, Can. J. Phys. 63 (1985) 826.
[56] J.P.M. Schmitt, J. Non-Cryst. Solids 59/60 (1983) 649.
[57] E.M. Horwitz, Appl. Surf. Sci. 22/23, Pt. 2 (1985) 925.
[58] H. Sugai, H. Toyoda, A. Yoshida and T. Okuda, Appl. Phys. Lett. 46 (1985) 1048.
[59] W.E. Spear and P.G. LeComber, in ref. [34], p. 63.
[60] K. Ebihara and S. Maeda, J. Appl. Phys. 57 (1985) 2482.
[61] M.P. Rosenblum, M.J. Thompson and R.A. Street, AIP Conf. Proc. 73, eds. R.A. Street, D.K. Biegelsen and J.C. Knights, (1981) p. 42.
[62] Y. Kuwano and M. Ohnishi, J. de Phys. 42, Coll. C4 (1981) 1155.
[63] M. Izo and S.R. Ovshinsky, Thin Solid Films 119 (1984) 59.
[64] H. Sakai, M. Maruyama, T. Yoshida, Y. Ichikawa, M. Kamiyama, T. Ichimura and Y. Uchida, Conf. Rec. IEEE Photovoltaic Spec. Conf. 17 (1984) 76.
[65] P.D. Richard, D.V. Tsu, G. Lucovsky and S.Y. Lin, J. Non-Cryst. Solids 77/78 (1985) 925.
[66] I. Kato, H.C. Card, K.C. Kao, S.R. Mejia and L. Chow, Rev. Sci. Instr. 53 (1982) 214.
[67] I. Kato, S. Wakana, S. Hara and H. Kezuka, Jpn. J. Appl. Phys. 21 (1982) L470.
[68] S. Kato and T. Aoki, J. Non-Cryst. Solids 77/78 (1985) 813.
[69] L. Paquin, D. Masson, M.R. Wertheimer and M. Moisan, Can. J. Phys. 63 (1985) 831.
[70] S.J. Hudgens, A.G. Johncock and S.R. Ovshinsky, J. Non-Cryst. Solids 77/78 (1985) 809.
[71] S.R. Mejia, R.D. McLeod, K.C. Kao and H.C. Card, J. Non-Cryst. Solids 59/60 (1983) 727.
[72] S.R. Mejia, R.D. McLeod, W. Pries, P. Shufflebotham, D.J. Thomson, J. White, J. Schellenberg, K.C. Kao and H.C. Card, J. Non-Cryst. Solids 77/78 (1985) 765.
[73] S.R. Mejia, R.D. McLeod, K.C. Kao and H.C. Card, Rev. Sci. Instr. 57 (1986) 493.
[74] J.J. Schellenberg, R.D. McLeod, S.R. Mejia, H.C. Card and K.C. Kao, Appl. Phys. Lett. 48 (1986) 163.
[75] C.A. Hewett, S.S. Lau, I. Suni and D.B. Poker, Nucl. Instr. and Meth. B7&8 (1985) 597.
[76] K.G. Prasad, M.B. Kurup and A. Bhagawat, Nucl. Instr. and Meth. B15 (1986) 698.
[77] A.V. Mirmel'shtein, A.E. Kar'lin, M.N. Khoplin and V.E. Arkhipov, Phys. Met. Metallogr. 60 (1985) 1025.
[78] W.E. Spear, P.G. Le Comber, S. Kalbitzer and G. Müller, Phil. Mag. B39 (1979) 159.
[79] W. Beyer, R. Fischer and H. Overhof, Phil. Mag. B 39 (1979) 205.
[80] D.J. Bishop, E.G. Spencer and R.C. Dynes, Sol. St. Elect. 28 (1985) 73.
[81] J.B. Holt, D.C. Ankeny and C.F. Cline, Scripta Met. 14 (1980) 959.
[82] D. Malterre, J. Durand and G. Marchal, J. Non-Cryst. Solids 61/62 (1984) 1137.
[83] N.T. Bagraev, L.S. Vlasenko and M.M. Mezdrogina, Sov. Tech. Phys. Lett. 7 (1981) 80.
[84] Y.-X. Zhao and D.L. Decker, Sol. St. Commun. 52 (1984) 889.
[85] P. Duwez, R.H. Willens and R.C. Crewdson, J. Appl. Phys. 36 (1965) 2267.
[86] U. Köster and P. Weiss, J. Non-Cryst. Solids 17 (1975) 359.
[87] G. Fritsch, W. Dyckhoff, W. Pollich and E. Lüscher, J. Phys. F: Met. Phys. 15 (1985) 1537.
[88] S.M. Filpek, A.W. Szafrański and P. Duhaj, J. Less Comm. Metals 101 (1984) 299.
[89] E. Huber, M. Von Allmen, Phys. Rev. B 28 (1983) 2979.
[90] K. Morigaki, Phil. Mag. B42 979 (1980).

[91] M. Dayan, N. Croitoru and Y. Lereah, Phys. Lett. A 82 306 (1981).
[92] T. Shimizu, M. Kumeda, I. Watanabe and Y. Noumi, Phil. Mag. B 44 (1981) 159.
[93] T. Luciński and J. Baszyński, Phys. Stat. Sol. A 87 (1985) K191.
[94] X. Le, C.L. Foiles and D.K. Reinhard, J. Non-Cryst. Solids 47 (1982) 355.
[95] R.W. Fane and Y. Zaka, J. Phys. D: Appl. Phys. 16 1993 (1983).
[96] L. Xu, C.L. Foiles and D.K. Reinhard, Phil. Mag. B 49 (19840 249.
[97] A.D. Inglis, J.R. Dutcher, N. Savvides, S.P. McAlister and C.M. Hurd, Sol. St. Commun. 47 (1983) 555.
[98] M. Audier, P. Guyot, J.P. Simon and N. Valignat, J. de Phys. 46, Coll. C4 (1985) 433.
[99] E. Huber and M. von Allmen, Phys. Rev. B 31 (1985) 3338.
[100] K.V. Rao, in ref. [7], p. 401.
[101] P. Svoboda and P. Vašek, J. Phys. F: Met. Phys. 15 (1985) 2489.
[102] S.B. Dierker, H. Gudmundsson and A.C. Anderson, Sol. St. Commun. 29 (1979) 767.
[103] T. Luciński and J. Baszyński, Phys. Stat. Sol. A 84 (1984) 607.
[104] P. Mangin, G. Marchal, C. Mourey and C. Janot, Phys. Rev. B 21 (1980) 3047.
[105] U. Mizutani, Prog. Mater. Sci. 28, no. 2 (1983).
[106] A. Inoue, T. Masumoto and H.S. Chen, J. Phys. F: Met. Phys. 13 (1983) 2603.
[107] A.S. Edelstein, S.R. Ovshinky, H. Sadate-Akhavi and J. Wood, Sol. St. Commun. 41 (1982) 139.
[108] W. Wen-Kui, Chin. Phys. 5 (1985) 581.
[109] C. Suryanarayana, A. Inoue and T. Masumoto, J. Mater. Sci. 15 (1980) 1993.
[110] K. Akitmoto and K. Watanabe, Appl. Phys. Lett. 39 (1981) 445.
[111] R.H. Crewsdon, Calif. Tech. Rep. CALT-221-20 (1966) p. 21.
[112] N.F. Mott, Metal–Insulator Transitions (Taylor & Francis, London, 1974).
[113] N.F. Mott and M. Kaveh, Adv. Phys. 34 (1985) 329.
[114] Sol. St. Elect. 28, nos. 1/2 (1985).
[115] N. Nishida, T. Furubayashi, M. Yamaguchi, K. Morigaki and H. Ishimoto, Sol. St. Elect. 28 (1985) 81.
[116] A. Möbius, H. Vinzelberg, C. Gladun, A. Heinrich, D. Elefant, J. Schumann and G. Zies, J. Phys. C: Sol. St. Phys. 18 3337 (1985).
[117] J.C. Slater, Quantum Theory of Molecules and Solids, Vol. 2 (McGraw–Hill, New York, 1965).
[118] M.M. Collver, Sol. St. Commun. 23 (1977) 333.
[119] A. Möbius, J. Phys. C: Sol. St. Phys. 18 (1985) 4639.
[120] A. Hiraki, A. Shimizu, M. Iwami, T. Narusawa and S. Komiya, Appl. Phys. Lett. 26 (1975) 57.
[121] K. Murase, A. Takeda and Y. Mizushima, Jpn. J. Appl. Phys. 21 (1982) 561.
[122] W. Buckel and R. Hilsch, Z. Physik 138 (1954) 109, 118.
[123] S.J. Poon, in ref. [7], p. 432.
[124] B. Strizker and H.L. Luo, J. Less Com. Metals 73 (1980) 301.
[125] Z. Qirui and H.C. Freyhardt, Chin. Phys. 5 (1985) 1019.
[126] N. Nishida, M. Yamaguchi, T. Furubayashi, K. Morigaki, H. Ishimoto and K. Ono, Sol. St. Commun. 44 (1982) 305.
[127] D. Dew-Hughes and V.D. Linse, J. Appl. Phys. 50 (1979) 3500.
[128] C.C. Tsuei, Appl. Phys. Lett. 33 (1978) 262.
[129] T. Masumoto, A. Inoue, S. Sakai, H. Kimura and A. Hoshi, Trans. Jpn. Inst. Met. 21 (1980) 115.
[130] C. Suryanarayana, W.K. Wang, H. Iwasaki and T. Masumoto, Sol. St. Commun. 34 (1980) 861.
[131] G. Wei-Yan, C. Xi-Shen, W. Zu-Lun, Y. Sun-Sheng and L. Ying, Acta Phys. Sin. 31 (1982) 485 (in Chinese).
[132] Y. Kuwano and S. Tsuda, in ref. [46], p. 108.
[133] C.J. Mogab and W.D. Kingery, J. Appl. Phys. 39 (1968) 3640.
[134] E.A. Fagen, in: Amorphous and Liquid Semiconductors, Vol. 1 eds. J. Stuke, W. Brenig (Taylor & Francis, London, 1973) p. 601.

[135] K. Nair and S.S. Mitra, J. Non-Cryst. Solids 24 (1977) 1.
[136] D.A. Anderson and W.E. Spear, Phil. Mag. 35 (1977) 1.
[137] D. Caffier, M. Le Contellec and J. Richard, J. de Phys. Coll. C4, 42, Suppl. 10 (1981) 1037.
[138] R.S. Sussmann and R. Ogden, Phil. Mag. B 44 (1981) 137.
[139] Y. Tawada, K. Tsuge, M. Kondo, H. Okamoto and Y. Hamakawa, J. Appl. Phys. 53 (1982) 5273.
[140] I. Watanabe, Y. Hata, A. Morimoto and T. Shimizu, Jpn. J. Appl. Phys. 21 (1982) L613.
[141] A. Morimoto, T. Miura, M. Kumeda and T. Shimizu, J. Appl. Phys. 53 (1982) 7299.
[142] J. Bullot, M. Gauthier, M. Schmidt, Y. Catherine and A. Zamouche, Phil. Mag. B 49 (1984) 489.
[143] A.H. Mahan, D.L. Williamson, M. Ruth and P. Rabiosson, J. Non-Cryst. Solids 77/78 (1985) 861.
[144] Y. Catherine and G. Turban, Thin Sol. Films 60 (1979) 193; ibid. 70 (1980) 101.
[145] T.E. Hartman, I.C. Blair and C.A. Mead, Thin Solid Films 2 (1968) 79.
[146] D.D. Allred, D.C. Booth, B.R. Appleton, P.D. Miller, C.D. Moak, J.P.F. Sellschop, C.W. White and A.L. Wintenberg, IEEE Trans. Nuclear Sci. NS-28 1838 (1981).
[147] R. Dutta, P.K. Banerjee and S.S. Mitra, Phys. Stat. Sol. B 113 (1982) 277.
[148] S. Iida and S. Ohki, Jpn. J. Appl. Phys. 21 (1982) L62.
[149] T. Shimada, Y. Katayama and K.F. Komatsubara, J. Appl. Phys. 50 (1979) 5530.
[150] N. Saito, J. Appl. Phys. 58 (1985) 3504.
[151] M. Le Contellec, J. Richard, A. Guivarch, E. Ligeon and J. Fontenille, Thin Solid Films 58 (1979) 407.
[152] B. Abeles, T. Tiedje, K.S. Liang, H.W. Deckman, H.C. Stasiewski, J.C. Scanlon, P.M. Eisenberger, J. Non-Cryst. Solids 66 (1984) 351.
[153] D. Engeman, R. Fischer and J. Knecht, Appl. Phys. Lett. 32 (1978) 567.
[154] A. Yamada, J. Kenne, M. Konagai and K. Takahashi, Appl. Phys. Lett. 46 (1985) 272.
[155] Y. Katayama, T. Shimada and K. Usami, Phys. Rev. Lett. 46 (1981) 1146.
[156] Y.-Y. Lee, J. Appl. Phys. 51 (1980) 3365.
[157] R. Dutta, P.K. Banerjee and S.S. Mitra, Phys. Rev. B 27 (1983) 5032.
[158] H. Munekata, A. Shiozaki and H. Kukimoto, J. Lumin. 24/25 (1981) 43.
[159] H. Munekata and H. Kukimoto, Appl. Phys. Lett. 42 (1982) 432.
[160] H. Matsunami, M. Yoshimoto, Y. Fujii and J. Saraie, J. Non-Cryst. Solids 59/60 (19830 569.
[161] A. Onton, H. Wiecker, D. Chevallier and C.R. Guarnieri, in: Proc. 7th Int. Conf. on Amorphous and Liquid Semiconductors, Edinburgh, ed. W.E. Spear (Stevenson, Edinburgh, 1977) p. 357.
[162] D. Hauschildt, R. Fischer and W. Fuhs, Phys. Stat. Sol. B 102 (1980) 563.
[163] G. Nakamura, K. Sato, H. Kondo, Y. Yukimoto and K. Shirahata, J. de Phys. Coll. C4, 42 Suppl. 10 (1981) 483.
[164] M.C. Cretella and J.A. Gregory, J. Electrochem. Soc. 129 (1982) 2850.
[165] B. von Roedern, D.K. Paul, J. Blake, R.W. Collins, G. Moddel and W. Paul, Phys. Rev. B 25 (1982) 7678.
[166] G. Nakamura, K. Sato and Y. Yukimoto, Solar Cells 9 (1983) 75.
[167] L. Chahed, C. Senemaud, M.L. Theye, J. Bullot, M. Galin, M. Gauthier, B. Bourdon and M. Toulemonde, Sol. St. Commun. 45 (1983) 649.
[168] J. Bullot, M. Galin, M. Gauthier and B. Bourdon, J. de Phys. 44 (1983) 713.
[169] C.Y. Huang, S. Guha and S.J. Hudgens, J. Non-Cryst. Solids 66 (1984) 187.
[170] J. Chevallier, H. Wieder, A. Onton and C.R. Guarnieri, Sol. St. Commun. 24 (1977) 867.
[171] W. Paul, D.K. Paul, B. von Roedern, J. Blake and S. Oguz, Phys. Rev. Lett. 46 (1981) 1016.
[172] A. Morimoto, T. Miura, M. Kumeda and T. Shimizu, Jpn. J. Appl. Phys. 20 (1981) L833.
[173] T. Ichimura, T. Ihara, T. Hama, M. Ohsma, H. Sakai and Y. Uchida, J. Non-Cryst. Solids 77/78 (1985) 901.
[174] K.D. Mackenzie, J.R. Eggert, D.J. Leopold, Y.M. Li, S. Lin and W. Paul, Phys. Rev. B 31 (1985) 2198.

[175] I. Shimizu, in ref. [46], p. 300.
[176] K.D. Mackenzie, J. Hanna, J.R. Eggert, Y.M. Li, Z.L. Sun and W. Paul, J. Non-Cryst. Solids 77/78 (1985) 881.
[177] N. Van Dong, T.H. Danh and J.Y. Leny, J. Appl. Phys. 52 (1981) 338.
[178] P.K. Banerjee, R. Dutta and S.S. Mitra, J. Non-Cryst. Solids 50 (1982) 1.
[179] K.C. Kao, R.D. McLeod, C.H. Leung, H.C. Card and H. Watanabe, J. Phys. D: Appl. Phys. 16 (1983) 1801.
[180] R.A. Rudder, G.N. Parsons, J.W. Cook Jr. and G. Lucovsky, J. Non-Cryst. Solids 77/78 (1985) 885.
[181] S.Z. Weisz, M. Gomez, J.a. Muir, O. Rest. R. Perez, Y. Goldstein and B. Abeles, Appl. Phys. Lett. 44 (1984) 634.
[182] H. Itozaki, N. Fujita and H. Hitotsuyanagi, Mat. Res. Symp. Proc. 49 (1985) 161.
[183] D. Beaglehole and M. Zavetova, J. Non-Cryst. Solids 4 (1970) 272.
[184] D.L. Staebler and C.R. Wronski, J. Appl. Phys. 51 (1980) 3262.
[185] C.R. Wronski and R.E. Daniel, Phys. Rev. B 23 (1981) 794.
[186] C. Vérié, J.F. Rochette and J.P. Rebouillat, J. de Phys. Coll. C4, 42, Supp. 10 (1981) 667.
[187] M. Vergnat, M. Peicuch, G. Marchal and M. Gerl, Phil. Mag. B 51 (1985) 327.
[188] A.H. Mahan, D.L. Williamson and A. Madan, Appl. Phys. Lett 44 (1984) 220.
[189] B. Von Roedern, A.H. Madan, R. Könenkamp, D.L. Williamson, A. Sanchez and A. Madan, J. Non-Cryst. Solids 60 (1984) 13.
[190] Y. Kuwano, M. Ohnichi, H. Nishiwaki, S. Tsuda, F. Fukatsu, K. Enomoto, Y. Nakashima and H. Tarui, Conf. Rec. IEEE Photovoltaic Spec. Conf. 16 (1982) 1338.
[191] D.L. Williamson and S.K. Deb, J. Appl. Phys. 54 (1983) 2588.
[192] A. Morimoto, T. Kataoka and T. Shimizu, Jpn. J. Appl. Phys. 24 Pt.1 (1985) 1122.
[193] A.A. Andreev, O.A. Golikova, F.S. Nasredinov, P.V. Nistiryuk and P.P. Seregin, Sov. Phys.: Semicond. 16 (1982) 715.
[194] J. Baixeras, D. Mencaraglia and P. Andro, Phil. Mag. 37 (1978) 403.
[195] B. Dunnet, D.I. Jones and A.D. Stewart, Phil. Mag. B 53 (1986) 159.
[196] A.J. Lowe, M.J. Powell and S.R. Elliot, J. Appl. Phys. 59 (1986) 1251.
[197] Y. Nishibayashi, T. Imura and Y. Osaka, J. Non-Cryst. Solids 77/78 (1985) 941.
[198] A. Chayahara, M. Ueda, T. Hamasaki and Y. Osaka, Jpn. J. Appl. Phys. 24 Pt. 1 (1985) 19.
[199] R.W. Griffith, F.J. Kampas, P.E. Vanier and M.D. Hirsch, J. Non-Cryst. Solids 35/36 (1980) 391.
[200] H. Watanabe, K. Katoh and M. Yasui, Jpn. J. Appl. Phys. 21 (1982) L341.
[201] H. Watanabe, K. Katoh and M. Yasui, Thin Solid Films 106 (1983) 263.
[202] H. Watanabe, K. Katoh, M. Yasui and Y. Shibata, J. Non-Cryst. Solids 59/60 (1983) 605.
[203] H. Watanabe, K. Katoh and M. Yasui, Jpn. J. Appl. Phys. 23 (1984) 1.
[204] T.V. Herak, R.D. McLeod, K.C. Kao, H.C. Card, H. Watanabe, M. Katoh, M. Yasui and Y. Shibata, J. Non-Cryst. Solids 69 (1984) 39.
[205] T.V. Herak, R.C. McLeod, M.G. Collett, K.C. Kao, H.C. Card, H. Watanabe, M. Katoh, M. Yasui and Y. Shibata, Can. J. Phys. 63 (1985) 846.
[206] W.Y. Xu, Z.L. Sun, Z.P. Wang and D.L. Lee, J. de Phys. Coll. C4, 42, Supp. 10 (1981) 695.
[207] S.M. Pietruszko, K.L. Narasimhan and S. Guha, Phil. Mag. 43 (1981) 357.
[208] H. Kurata, M. Hirose and Y. Osaka, Jpn. J. Appl. Phys. 20 (1981) L811.
[209] T. Noguchi, S. Usui, A. Sawada, Y. Kanoh and M. Kikuchi, Jpn. J. Appl. Phys. 21 (1982) L485.
[210] G. Sasaki, M. Kondo, S. Fujita and A. Sasaki, Jpn. J. Appl. Phys. 21 (1982) 1394.
[211] P.D. Richard, D.V. Tsu, G. Lucovsky and S.Y. Lin, J. Non-Cryst. Solids 77/78 (1985) 925.
[212] G. Sasaki, S. Fujita and A. Sasaki, Appl. Phys. Lett. 54 (1983) 2696.
[213] G. Lucovsky and W.B. Pollard, in: Topics in Applied Physics 56, The Physics of Hydrogenated Amorphous Silicon II, eds. J.D. Joannopoulos, G. Lucovsky (Springer, Berlin, 1984) p. 301.
[214] C.C. Tsai, Phys. Rev. B 19 (1979) 2041.
[215] J.C. Knights, Phil. Mag. 34 (1976) 663,

[216] D. Leidich, E. Linhart, E. Niemann, H.W. Grueninger, R. Fischer and R.R. Zeyfang, J. Non-Cryst. Solids 59/60 (1983) 613.
[217] B.G. Yacobi, R.W. Collins, G. Moddel, P. Viktorovitch and W. Paul, Phys. Rev. Lett. B 24 (1981) 5907.
[218] P.K. Shufflebotham, H.C. Card, K.C. Kao and A. Thanailakis, J. Appl. Phys. 60 (1986) 2036.
[219] F.A. Faris, A. Al-Jassar, F.G. Wakim and K.Z. Botros, Mat. Res. Soc. Symp. Proc. 49 (1985) 225.
[220] K.E. Peterson, U. Birkholz and D. Adler, Phys. Rev. B 8 (1973) 1453.
[221] H.S. Chen, C.E. Miller, Rev. Sci. Instr. 41 (1970) 1237.
[222] P. Lamparter, A. Habenschuss and A.H. Narten, J. Non-Cryst. Solids 86 (1986) 109.
[223] F.G. Wakim, A. Al-Jassar and S.A. Abo-Namous, J. Non-Cryst. Solids 53 (1982) 11.
[224] F.G. Wakim, A. Al-Jassar, M.A. Hassan and K.Z. Botros, J. Non-Cryst. Solids 59/60 (1983) 617.
[225] F.G. Wakim, s.A. Abo-Namous, A. Al-Jassar and M.A. Hassan, Appl. Phys. Lett. 42 (1983) 523.
[226] F.R.L. Schoening, J. Mater. Sci. 14 (1979) 2397.
[227] G.E.A. Bartsch, H. Bromme and T. Just, J. Non-Cryst. Solids 18 (1975) 65.
[228] S.A. Altunyan, V.s. Miinaev, M.S. Minazhdinov and B.K. Sachkov, Sov. Phys.: Semicond. 4 (1971) 1906.
[229] A. Madan, in ref. [34], p. 245.
[230] A. Madan, W. Czybatyj, J. Yang, J. McGill and S.R. Obshinsky, J. de Phys. 42 Coll. C4 (1981) 463.
[231] S.R. Ovshinsky and D. Adler, Mat. Res. Soc. Symp. Proc. 49 (1985) 251.
[232] S. Al Dallal, S. Kalem, J. Boureix, J. Chevallier and M. Toulemonde, Phil. Mag. B 50 (1984) 493.
[233] K. Murase and Y. Mizushima, in ref. [46], p. 242.
[234] K. Murase, Y. Amemiya and Y. Mizushima, Jpn. J. Appl. Phys. 21 (1982) 1559.
[235] A. Morimoto, S. Takamori and T. Shimizu, J. Non-Cryst. Solids 77/78 (1985) 965.
[236] Y. Tawada, M. Kondo, H. Okamoto and Y. Hamakawa, Conf. Rec. IEEE Photovoltaic Spec. Conf. 15 (1981) 245.
[237] H. Kukimoto, in ref. [3], p. 239.
[238] D.E. Carlson, in ref. [3], p. 7.
[239] Y. Uchida, in ref. [46], p. 180.
[240] Y. Hamakawa and H. Okamoto, in ref. [46], p. 200.
[241] H. Morimoto and M. Izu, in ref. [46], p. 212.
[242] Y. Kuwano and S. Nakano, in ref. [46], p. 222.
[243] D.E. Carlson and C.R. Wronski, in: Amorphous Semiconductors, ed. M.H. Brodsky (Springer, Berlin, 1981) p. 287.
[244] D.E. Carlson, U.S. Patent 4,064,521 (1977).
[245] S. Nakano, Y. Kishi, M. Ohnishi, S. Tsuda, H. Shibuya, N. Nakamura, Y. Hishikawa, H. Tarui, T. Takahama and Y. Kuwano, Mat. Res. Soc. Symp. Proc. 49 (1985) 275.
[246] Y. Hamakawa, Mat. Res. Soc. Symp. Proc. 49 (1985) 239.
[247] G. Nakamura, K. Sato, H. Kondo, Y. Yukimoto and K. Shirahata, in: 4th Eur. Comm. Photovoltaic Sol. Energy Conf., Stresa, Italy (Reidel, Dordrecht, Holland, 1982) p. 616.
[248] A. Catalano, R.V. D'Aiello, J. Dresner, B. Faughnan, A. Firester, J. Kane, H. Schade, Z.E. Smith, G. Schwartz and A. Triano, Conf. Rec. IEEE Photovoltaic Spec. Conf. 16 (1982) 1421.
[249] G. Nakamura, K. Sato, T. Ishihara, M. Usui, K. Okaniwa and Y. Yukimoto, J. Non-Cryst. Solids 59/60 (1983) 1111.
[250] C. Vérié, Conf. Rec. IEEE Photovoltaic Spec. Conf. 17 (1984) 245.
[251] S. Wiedeman and E.A. Fagen, Conf. Rec. IEEE Photovoltaic Spec. Conf. 17 (1984) 223.
[252] E. Sabisky, W. Wallace, B. Stafford, K. Sadlon and W. Luft, Mat. Res. Soc. Symp. Proc. 49 (1985) 281.

[253] S. Guha, J. Non-Cryst. Solids 77/78 (1985) 1451.
[254] M. Matsumura, in ref. [46], p. 236.
[255] D.H. Auston, P. Lavallard, N. Sol and D. Kaplan, Appl. Phys. Lett. 36 (1980) 66.
[256] P.G. LeComber and W.E. Spear, in ref. [3], p. 89.
[257] Y. Hirai, K. Sakai, Y. Osada, K. Aihara and T. Nakagiri, J. Non-Cryst. Solids 59/60 (1983) 1191.
[258] A.J. Snell, P.G. Le Comber, K.D. MacKenzie, W.E. Spear and A. Doghmane, J. Non-Cryst. Solids 59/60 (1983) 1187.
[259] M. Matsumura, in ref. [3], p. 161.
[260] N. Harada, in ref. [46], p. 283.
[261] S. Kishida, Y. Naruke, Y. Uchida and M. Matsumara, J. Non-Cryst. solids 59/60 (1983) 1281.
[262] D.G. Ast, in ref. [3], p. 115.
[263] M. Ghannam, J. Nijs, R. De Keersmaecker and R. Mertens, Mat. Res. Soc. Symp. Proc. 49 (1985) 437.
[264] S. Kaneko, in ref. [3], p. 139.
[265] T. Tsukada, in ref. [46], p. 290.
[266] A. D'Amico and G. Fortunato, in ref. [3], p. 209.
[267] P.G. LeComber, Mat. Res. Soc. Symp. Proc. 49 (1985) 341.
[268] A.J. Snell, A. Doghmane, P.G. LeComber and W.E. Spear, Appl. Phys. A 34 (1984) 175.
[269] P.G. LeComber, A.J. Snell, K.D. MacKenzie and W.E. Spear, J. de Phys. 42, Coll. C4 (1981) 423.
[270] M. Matsumura, H. Hayama, Y. Nara and K. Ishibashi, IEEE Elect. Dev. Lett. 1 (1980) 182.
[271] A.J. Snell, W.E. Spear, P.G. LeComber and K.D. MacKenzie, Appl. Phys. A 26 (1981) 83.
[272] A.E. Owen, P.G. LeComber, G. Sarrabayrouse and W.E. Spear, IEEE Proc. 129 (1982) 51.
[273] A.E. Owen, P.G. LeComber, W.E. Spear and J. Hajto, J. Non-Cryst. Solids 59/60 (1983) 1273.
[274] P.G. LeComber, A.E. Owen, W.E. Spear, J. Hajto and W.K. Choi, in ref. [3], p. 275.
[275] M. Yamano and H. Takesada, J. Non-Cryst. Solids 77/78 (1985) 1381.
[276] M. Tsukude, S. Akamatsu, M. Hirose and M. Ueda, J. Non-Cryst. Solids 77/78 (1985) 1389.
[277] I. Shimizu, in ref. [3], p. 55.
[278] I. Shimizu, Mat. Res. Soc. Symp. Proc. 49 (1985) 395.
[279] I. Shimizu, J. Non-Cryst. Solids 77/78 (1985) 1363.
[280] S. Ishioka, in ref. [3], p. 75.
[281] R.J. Phelan Jr., in ref. [3], p. 249.
[282] S. Nishikawa, H. Kamimura, T. Watanabe and K. Kaminishi, J. Non-Cryst. Solids 59/60 (1985) 1235.
[283] S. Ishioka, Y. Imamura, Y. Takasaki, C. Kusano, T. Hirai and S. Nobitoki, Jpn. J. Appl. Phys. 22, Pt. 1 (1983) 461.
[284] I. Inoue, T. Tanaka, M. Konagai and K. Takahashi, Appl. Phys. Lett. 44 (1984) 871.
[285] S.J. Hudgens and A.G. Johncock, Mat. Res. Soc. Symp. Proc. 49 (1985) 403.
[286] De Kruangam, T. Endo, W. Guang-Pu, S. Nonomura, H. Okamoto and Y. Hamakawa, J. Non-Cryst. Solids 77/78 (1985) 1429.
[287] W. Wang, J. Non-Cryst. Solids 77/78 (1985) 1437.
[288] M.A. Bosch, in ref. [3], p. 173.
[289] R.D. McLeod, W. Pries, H.C. Card and K.C. Kao, Appl. Phys. Lett. 45 (1984) 628.
[290] J.M. Berger, J.P. Ferraton, B. Yous and A. Donradieu, Thin Solid Films 86 (1981) 337.
[291] S. Kodata, S. Nishida, M. Konagai and K. Takahashi, J. Non-Cryst. Solids 59/60 (1983) 1207.
[292] K. Murase, T. Tamanna, M. Sukave, T. Ogino, Y. Amemiya and Y. Mizushima, J. Non-Cryst. Solids 59/60 (1983) 1211.